

Date: June 16, 2017

EIC Detector R&D Progress Report

Project ID: eRD6

Project Name: Tracking and PID detector R&D towards an EIC detector

Period Reported: from January 2017 to July 2017

Project Leader:

Bonn University: Jochen Kaminski

Brookhaven National Lab: Craig Woody

DESY: Ties Behnke

Florida Tech: Marcus Hohlmann

INFN Trieste: Silvia Dalla Torre

Stony Brook University: Klaus Dehmelt, Thomas Hemmick

University of Virginia: Kondo Gnanvo, Nilanga Liyanage

Yale University: Richard Majka, Nikolai Smirnov

Contact Person: Klaus Dehmelt

Project members:

Bonn University: K. Desch, J. Kaminski

Brookhaven National Lab: B. Azmoun, M. L. Purschke, C. Woody

Brookhaven National Lab - Medium energy group: E. C. Aschenauer, A. Kiselev

DESY: T. Behnke, R. Diener, U. Einhaus

Florida Tech: M. Hohlmann

INFN Trieste: S. Dalla Torre

Stony Brook University: K. Dehmelt, A. Deshpande, N. Feege, T. K. Hemmick, P. Garg

University of Virginia: K. Gnanvo, N. Liyanage

Yale University: R. Majka, N. Smirnov

Contents

EIC Detector R&D Progress Report	1
Vision for eRD3/eRD6.....	4
Past.....	6
What was planned for this period?	6
Brookhaven National Lab	6
Florida Tech	7
INFN Trieste	7
Stony Brook University:	8
Univ. of Virginia	8
What was achieved?	9
Brookhaven National Lab	9
Florida Tech	13
INFN Trieste	16
Stony Brook University:	21
Univ. of Virginia	21
Yale University	26
What was not achieved, why not, and what will be done to correct?	27
Brookhaven National Lab	27
Florida Tech	27
INFN Trieste	27
Stony Brook University:	27
Univ. of Virginia	27
Future.....	28
Brookhaven National Lab	28
Florida Tech	28
INFN Trieste	28
Stony Brook University:	29
Univ. of Virginia	29
Yale University	29
What are critical issues?.....	29
Brookhaven National Lab	29
Florida Tech	30
INFN Trieste	30
Stony Brook University:	30
Univ. of Virginia	30
Yale University	30
Manpower	30
Brookhaven National Lab	30

Florida Tech	30
INFN Trieste	30
Stony Brook University:	31
Univ. of Virginia	31
Yale University	31
External Funding	31
Brookhaven National Lab	31
Florida Tech	31
INFN Trieste	31
Stony Brook University:	31
Univ. of Virginia	32
Yale University	32
Publications	32
Brookhaven National Lab	32
Florida Tech	32
INFN Trieste	32
Stony Brook University:	32
Univ. of Virginia	33
Proposals	34
Brookhaven National Lab	34
Zigzag pad development	34
GEM-based cosmic ray telescope	34
GEM Studies using TPC gas mixtures (collaborate with Stony Brook group)	34
Joint R&D Proposal from Florida Tech and UVA	34
Beam Test of EIC-FT GEM prototypes at Fermilab (spring / summer 2018)	34
Development of large-area chromium GEM foil	35
Development of cylindrical μ -RWELL detectors for acquiring fast hit information in the central EIC tracking detector	35
Stony Brook University	37
Ion BackFlow Studies	37
Joint R&D Proposal Stony Brook University/Bonn University/DESY	43
Funding requests and budget	51
Proposed Budget for the BNL R&D program for FY18	51
Proposed Budget for the joint Florida Tech and UVA R&D program for FY18	52
UVA	52
Florida Tech	52
Cost reductions in -20% and -40% scenarios:	53
Funding Requests for INFN	53
Proposed Budget Request TPC IBF Studies	54
Proposed Budget for the joint Bonn University/DESY/SBU R&D program for FY18	54

Vision for eRD3/eRD6

The eRD3/eRD6 collaboration(s) were among the first few funded proposals for EIC R&D. As such the original directions of our research efforts were formulated before guidance was available from the now mature understanding of the EIC capabilities, challenges, and requirements. Our original R&D goals are, one-by-one, being completed (Yale 3-coordinate readout – done, SBU CsI RICH – done, BNL mini-drift – done, ...) and we are now seeking to initiate the next wave of studies.

To refresh and refocus our efforts to be most appropriate to the current understanding of EIC needs, we held a two-day workshop at Temple University in May 2017. In addition to representation from all our member institutions, we hosted invited talks on calorimetry, silicon tracking, EIC physics rates/requirements, and anticipated backgrounds. Specific detector designs including BeAST, the J-Lab EIC detector, and ePHENIX were discussed as a means of building a fresh generic picture of the EIC tracking needs and to discover new avenues for our next stages of research. Prior to presenting the institution-by-institution progress reports, we wish to summarize the findings of the Temple Meeting and indicate how this has inspired the current funding proposal.

Following the series of excellent presentations, a free form brainstorming session yielded the hand-drawn picture from Figure 1.

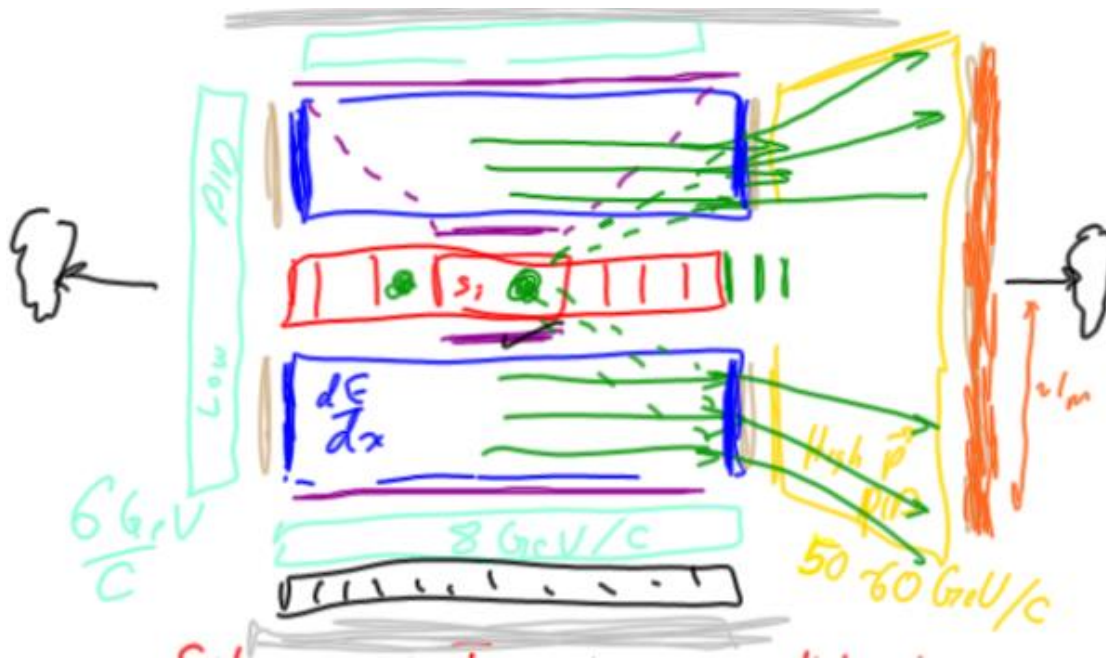


Figure 1 A generic conceptual design for the EIC tracking systems.

The various parts of the system follow a color code to distinguish among their capabilities. Although cartoonish in nature, we believe that this figure represents the best and most up-to-date summary of the EIC tracking requirements. The paragraphs below detail the various color-coded aspects of the tracking system and are followed by a short table for reference.

The red sections represent silicon-based tracking. Silicon tracking is currently that best single-point-resolution technology on the market and thereby a vital component nearest to the collision point for providing displaced vertex measurements as a means of studying heavy flavor quark production. When the incident electron is scattered toward mid rapidity, it is rather soft and therefore reconstruction of the correct event kinematics places strong restrictions on the material budget of the silicon tracker. Currently the MAPS technology being developed for the ALICE experiment is the best suited for an EIC application as these sensors (known as ALPIDE short for ALice Pixel DEtector) boast a pixel size of $28 \times 28 \mu\text{m}^2$ and a thickness of only 0.3% of a radiation length per layer. This technology, however, has a drawback by being integrating in nature. The latency of the detector is somewhat complicated to calculate since the device operates by a “raise your

hand when hit” principle. In ALICE, this integration period is more than a μsec . At EIC, it will be governed by the total hit rate, including machine background, which could be severe near to the beam pipe.

The blue section is a large-volume-gas-tracker. Gas remains the thinnest detector and various options exist including a drift chamber, straw tube chamber, or TPC. The principle deliverables from this device are superb pattern recognition and specific ionization measurements. Our group considers the options of straw tubes or TPC to be superior choices to a volume drift chamber and would not pursue this last choice. Although it has been correctly argued that a volume drift chamber could leverage cluster-counting to significantly improve dE/dx resolution, this involves the risk of wire breakage which can disable large regions of the detector and would likely require a long shutdown for repair. Conversely, straw tube chambers have been shown to be operable up to 2 atmospheres absolute pressure by the PANDA experiment, thereby doubling the ionization density while retaining all the advantages of cluster counting. The cost in material budget is well within EIC requirements (about 1% for 40 cm of detector in PANDA). Recent theoretical calculations have indicated that even in the case of long drift for a TPC, wherein diffusion can diminish the cluster counting efficacy, one nonetheless retains excellent dE/dx performance up to the loss of 80% of the clusters due to merging. Our R&D will be targeted at this latter effect, following the model of re-using the sPHENIX TPC for EIC. It should be noted that the sPHENIX TPC as designed is woefully inappropriate for the EIC. That device, in a quest to minimize space charge distortions, has effectively ruined dE/dx measurements in favor of momentum measurements. Furthermore, driven by present technology limits, the readout electronics shall be far thicker than appropriate for EIC application. To good approximation, one can salvage the field cage, but at a minimum (1) change the gas, (2) replace all avalanche stages at the electron arm, and (3) the innermost ring of avalanche stages in the hadron arm. Our R&D program shall focus on these modifications to the sPHENIX TPC to quantify the comparison of this technology to PANDA-like high pressure straws.

Because both the silicon MAPS and the TPC tracking solutions integrate collisions (and background) over multiple microseconds, one must surround these detectors with “fast taggers” as indicated by the purple lines sandwiching the TPC at its inner and outer radius. These fast taggers will provide the momentum resolution (as the TPC has been optimized for dE/dx) as well as sensitivity to only a single collision. Curved microMEGAS such as those recently deployed in the CLAS12 detector are an ideal technology for this function as they can provide $\sim 100\ \mu\text{m}$ resolution, low material budget, and the appropriately fast response.

The response of the volume tracker, regardless of technology, will be poor for high- η tracks that “clip the corner”. For this reason, planar GEM trackers as indicated by the tan lines should be placed at each endcap. Ideally these planar trackers would feature the mini-drift technology successfully investigated and developed by eRD6 so as to provide a track segment rather than a single point. Because the mini-drift is so short, at all EIC rates up to $10^{34}\ \text{cm}^{-2}\text{s}^{-1}$ luminosity these devices still provide single event tagging and verification to the slower detectors. This finding reinvigorates our planar GEM detector research efforts and will allow these to change over time to match the envelope defined by the large volume tracker endcaps. This evolution in the geometrical constraints of the forward tracking is driven by the realization that particles scattered at the highest eta will necessary require silicon tracking precision (e.g. MAPS) to meet the physics goals.

As we turn our attention to the endcaps, we note another need for gas detector R&D. Taking MAPS again as the technology of choice for high eta tracking again requires that the technology be “backed up” by devices with single event response properties. This is especially true for the far forward angles. Here we mimic the implementation in the central barrel by introducing an intermediate gas tracker for pattern recognition among the layers of MAPS devices as indicated by the green lines in the cartoon. The chromium GEM technology would make for an ideal device, since even at high momentum one wishes to keep the multiple scattering below the pixel resolution. Therefore, we are reinvigorated to pursue and make robust the chromium GEMS.

Indicated by the gold color is the high performance forward RICH detector. This effort is already reinvigorated, by the inclusion of our colleagues from Trieste who bring the experience from the recent and successful RICH development for COMPASS into the EIC arena. One product of this experience is the realization that RICH technology in the presence of real backgrounds and weak rings from particles just above the Cherenkov threshold necessarily requires robust track seeds to solve the pattern recognition problem. Therefore, the RICH is ideally sandwiched between trackers that will provide the seeds for the rings. This leads to the orange line at the right of the cartoon figure as a compliment to the brown lines.

The orange line following the high precision RICH will require the large area planar tracking developments that have been a focus of efforts in eRD6. There is, however, a recent twist. Although the primary electrons is, for all practical purposes, never deflected so far as to enter the hadron arm, there are nonetheless secondary electrons from hadron decay that are vital to tag. The e^+e^- decay of the J/ψ is a valuable measurement and can only be made with electron tagging in

the hadron arm. Some of the eRD6 members have therefore joined with other colleagues to develop a forward TRD detector which is essentially accomplished by planar GEMS, operated as mini-drift, using a Xe-based gas mixture, all placed behind a TR photon radiator. That initiative, while benefitting dramatically from our past efforts requests funding under a different cover.

The following table briefly summarizes the refreshed EIC tracking components and indicates goals of our future efforts:

Color	Name	Deliverable	Favored Tech	Comment
Red	Silicon Pixels	Displaced Vertex	MAPS	Must be thinnest technology to remain consistent with soft electrons
Blue*	Volume Tracker	dE/dx, pattern recognition	TPC or high-pressure straws	R&D will pursue and determine viability of using reconfigured sPHENIX TPC
Purple**	Single Event Barrel Tagger	Single event response, momentum resolution	μ MEGAS	Consistent with eRD3 goals.
Brown*	Fast Endcap Tagger	Single event response, track stub.	Mini-drift GEM detector	Alteration to ongoing development, yields beampipe region to silicon.
Green*	Forward Tagger	Single event response, patt. recognition at extremely low mass	Chromium GEMs	Interstitial layers between MAPS devices with even less
Gold*	High mom. RICH	PID up to 50 GeV/c	COMPASS RICH Technology	Investigate new possibilities with diamond powder cathodes.
Orange**	RICH Seed Tagger	Seed point for RICH, eID for J/ ψ	TRD	Pursued under different cover.

Asterisk superscripts indicate the items consistent with the eRD6 past and/or proposed R&D efforts. Double-asterisks indicate the research topics whose funding request is made under a separate request with additional collaborators from Saclay (μ MEGAS) or J-Lab (TRD). We believe that this list of R&D topics along with an effort on MAPS external to our collaboration represents a comprehensive list of R&D relevant to EIC tracking and compatible with all current EIC integrated detector proposals.

Past

What was planned for this period?

Brookhaven National Lab

1. *Beam test results from TPC-Cherenkov prototype:* We planned to complete the few remaining minor tasks associated with analyzing the TPCC beam test data and present the results in a paper to be submitted to the IEEE Journal, Transaction on Nuclear Science (TNS).
2. *New ZZ PCB:* After further optimizing the design of the zigzag pattern for the sense plane of a TPC, we planned to have the multilayer readout PCB comprising the zigzag pattern designed and fabricated. Upon receiving the PCB from the manufacturer, we planned to carefully inspect it for accuracy of production, followed by testing the PCB in a quadruple GEM setup.
3. *New high-intensity x-ray scanner:* We planned to complete the assembly and commissioning of our new x-ray scanner.
4. *GEM studies with Ne based mixtures:* We planned to study various characteristics of an ALICE-style quadruple GEM in Ne-based gas mixtures, which have a particularly high ion mobility. The characteristics to be studied include the gas gain, stability, and energy resolution.
5. *FEE using SAMPA:* We planned to test a prototype front-end-electronics board containing the SAMPA electronics for a TPC readout.

Forward Tracker (FT) GEM detector development:

Our main goal for the last six months was to complete production of all components for the new one-meter-long FT GEM detector with zigzag readout, assemble it and put it through a battery of quality control tests modeled on the QC for the large GEM detectors of the CMS forward muon upgrade.

In parallel, we planned to finalize a publication on the results of the X-ray studies of small improved zigzag readout boards that were reported in the Jan. 2017 eRD6 report.

Reminder about the project and its relevance for the experiments at EIC

Particle identification of electrons and hadrons over a wide momentum range is a key ingredient for the physics program at EIC. One of the most challenging aspects is hadron identification at high momenta, namely above 6-8 GeV/c, where the only possibility is the use of Cherenkov imaging techniques with gaseous radiator. The overall constraints of the experimental set-ups at a collider impose a limited RICH detector length and to operate in a magnetic fringing field. Even if a complete principle design of a RICH for high momenta h-PID coping with these constraints has not yet been elaborated, the use of gaseous photon detectors is the most likely choice. The goal of our project is an R&D to further develop MPGD-based single photon detectors in order to establish one of the key components of the RICH for high momentum hadrons. This R&D has also some aspects synergic to the development of TPC sensors: the miniaturization of the read-out elements and the reduction of the ions backflow.

The starting point is the hybrid MPGD detectors of single photons developed for the upgrade of the gaseous RICH counter of the COMPASS experiment at CERN SPS. The detector architecture (Figure 2) consists of three multiplication stages: two THick GEMs (THGEM) layers, the first one coated with a CsI film and acting as a photocathode, followed by a MicroMegas (MM) multiplication stage. The two THGEMs are staggered: this configuration is beneficial both to reduce the Ion BackFlow (IBF) and to increase the maximum gain at which the detector can be operated exhibiting full electrical stability. These photon detectors can operate at gains of at least 3×10^4 and exhibit an IBF rate lower than 5%. The gas mixtures used are by Ar and CH₄, with a rich methane fraction in order to maximize the photoelectron extraction. An original element of the hybrid MPGD photon detector is the approach to a resistive MM by discrete elements (Figure 3), which has been triggered by the resistive MM developed for the ATLAS experiment at CERN LHC but presents substantial differences. The anode elements (pads) facing the micromesh are individually equipped with large-value resistors and the HV is provided, via these resistors, to the anode electrodes, while the micromesh is grounded. A second set of electrodes (pads parallel to the first ones) is embedded in the anode PCB: the signal is transferred by capacitive coupling to these

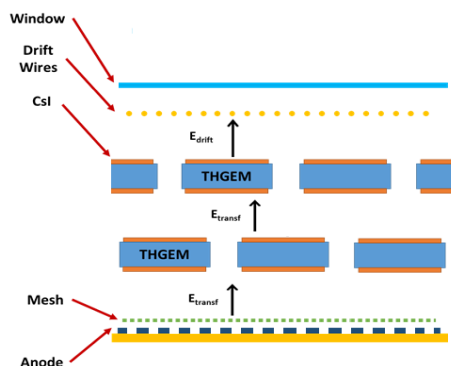


Figure 2 Schematic architecture of the hybrid MPGD detector of single photons (not to scale)

electrodes, which are connected to the front-end read-out electronics.

Stony Brook University:

An existing evaporator that is routinely used for evaporating CsI on GEMs for HBD like readout structures, will be upgraded with electron-gun and ion-beam equipment to precisely control the evaporation of material on surfaces of mirrors: the cover material of the mirror, Al and MgF₂ can be attached in a very controlled way to the surface of the prepared mirror blank.

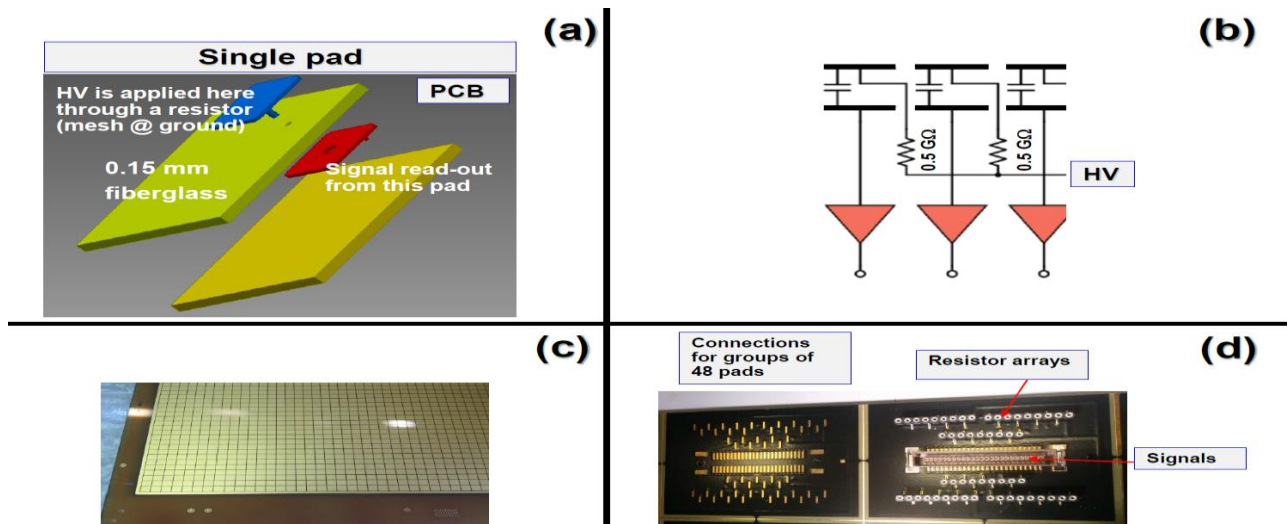


Figure 3 The resistive MM by discrete elements. (a) The principle is illustrated by a single pad; the different layer of the PCB forming the MM anode are schematically shown: the blue pad is the anode electrode of the MM kept at positive voltage; it directly faces the micromesh; the red pad is embedded in the PCB and the signal is transferred from the blue to the red pad by capacitive coupling. (b) The principle is illustrated by the electrical scheme: the top elements of the capacitors are the pad forming the MM anode (blue pad in (a)), the bottom elements of the capacitors (red pad in (a)) are connected to the front-end electronics. (c) Picture of the MM anode PCB in the present version, front view: the pad size is 8 x 8 mm². (d) Picture of the MM anode PCB in the present version, rear view, detail: the connectors serving 48 pads are grouped together; both the signal connectors and the supports of the resistor arrays are present.

Univ. of Virginia

R&D on Chromium GEM:

1. We plan to perform the long-term stability study of the Cr-GEM chamber in moderate background rate environment. We anticipate this test campaign to last over a couple of months for the results to be meaningful.
2. After the aging test is completed with Cr-GEM, perform high rate test of a hybrid GEM chamber with two Cr-GEM foils and Cr-Cu-GEM foil as the third foil at a high gain ($> 2 \times 10^4$). This would be a study to try to reproduce the degradation observed on third Cr-GEM foil in the first Cr-GEM prototype at extreme rate and gain and study the stability of the hybrid-Cr-GEM at high gain in high rate environment.
3. Inspection of the damaged Cr-GEM foil under SEM microscopy to acquire a high-resolution picture of the aging process and the radiation damage.

Assembly and characterisation the large EIC GEM prototype II:

1. Finalize the drawings of the U-V strip readout board and the zebra connection. Finalize the design of GEM support frames and the mechanical components of the full chamber.
2. Start the production of the U-V strips readout board at CERN and the GEM support frames soon after the funds become available
3. Plan for the assembly of the chamber and the characterization with Cosmic and X-ray as well as in test beam that we anticipate will likely be scheduled for the following funding cycle of July – December 2017.

Yale University

1. more measurements for 2 GEMs+MMG setup with R-protection
2. prepare multi-element stacked gated grid and get preliminary data

What was achieved?

Brookhaven National Lab

To prepare the final results from the beam test for publication, we spent time refining the analysis, mostly by incorporating more data files into the plots. The resulting position and angular resolutions for the two track angles measured (i.e., zero and three degrees) were very similar, where the corresponding residual

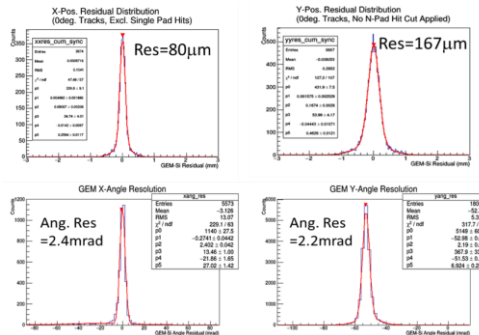


Figure 4 Top: X-coord. (along 2mm direction of pads) and Y-coord. (along field cage drift direction) resolution for zero degree inclined tracks. Bottom: Corresponding X and Y-coord. angular resolution.

distributions are shown for zero degrees in Figure 4. The tracks were reconstructed along two orthogonal planes, one parallel to the readout and the other parallel to the beam. For the x-position, tracks were reconstructed by determining a charge weighted average (i.e., centroid) of the charge deposited in each pad row. For the y-position, the charge arrival time was used to calculate coordinates along the drift direction of the field cage.

It should be noted that while the quoted position resolution in Figure 4 for the x-direction is quite good for a 2mm pad segmentation, the residual distributions shown here do not include single pad hits, which severely deteriorate the resolution. Roughly two-thirds of the collected events include single pad hits which are not reflected in the data shown. The single pad hits are due to the minimal transverse diffusion of pure CF_4 ($122\text{mm}/\sqrt{\text{cm}}$ at $400\text{V}/\text{cm}$ and 0 Tesla), the gas used for both the working gas of the TPC as well for the radiator of the Cherenkov portion of the detector, and the relatively poor interleaving of the older generation zigzag pads employed in this detector. The resolution along the y-direction was mostly limited by the relatively poor timing resolution of the APV25 electronics used to perform these measurements.

Additional analysis of data from the Cherenkov portion of the detector was also carried out. The plots in Figure 5 below show measurements of the photoelectron yield as a function of radiator length and as a function of the applied bias in the drift gap of the Cherenkov 4-GEM. Ultimately both measurements returned similar results, between 10 and 11 photoelectrons for a 29cm radiator length, in very good agreement with the expectation of about 12 photoelectrons.

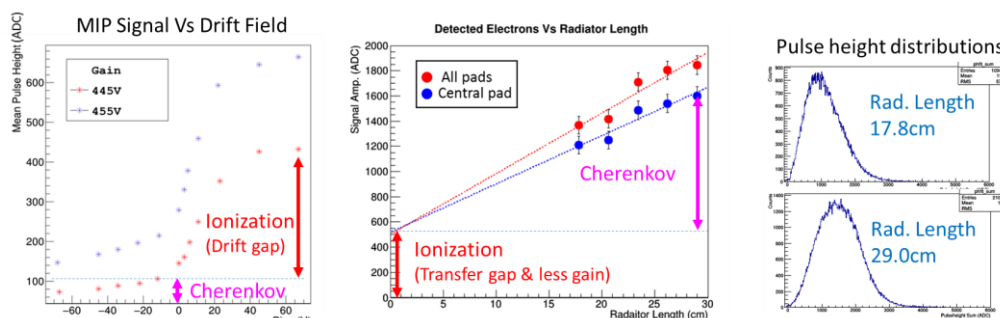


Figure 5 Cherenkov GEM bias scan vs Cherenkov signal. Middle: radiator length scan vs Cherenkov signal. Right: Pulse height distributions for two different radiator lengths. The specific ionization, which may be calculated based on known dE/dx values for CF_4 provides an absolute scale for the signal amplitude in terms primary photoelectrons.

Together with the Stony Brook group, we have also reported on the eID performance of the Cherenkov detector, using an external Cherenkov threshold trigger made available to us at the beam test facility. The resulting eID efficiency for the Cherenkov detector showed a 17% efficiency for detecting Kaons/protons, at 90% efficiency for detecting electrons/pions at gains approaching 10^4 .

These results were recently presented in a talk at the MPGD-2017 conference at Temple University in Philadelphia, PA. Also, a draft paper is currently being prepared for submission to IEEE Transaction on Nuclear Science, and we anticipate the submission date to be sometime this summer.

1. Zigzag GEM Readout (Note: the following work was done in collaboration with A. Kiselev, BNL Physics)

We have further optimized the parameters of the zigzag pattern in an effort to enhance charge sharing and to ensure a uniform response across the pad plane. We've designed a new multi-layer PCB to read out the zigzag pads and submitted the drawings to a PCB shop for fabrication. Upon receiving the new PCB, we inspected the PCB for the accuracy of fabrication and the results of this inspection are summarized in the tables in Figure 6.

In summary, the larger feature sizes, including the zigzag pitch and period were reproduced quite accurately, however, the smaller features like the trace and gap width had a margin of error approaching 5-10%. In particular, the zigzag geometry was distorted by both the over-etching of the zigzag tips and the trace width and by under-etching the zigzag troughs. The over-etched tips resulted in reducing the pad overlap from 94% in the design to 82% for the fabricated PCB. In addition, the area occupied by the copper conductor was diminished from 67% to 63%.

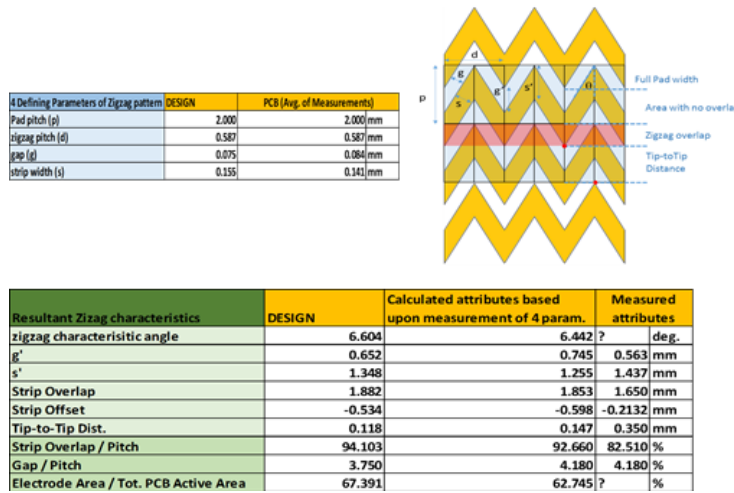


Figure 6 Structural characteristics of the zigzag pads of the new GEM readout PCB: design vs measured features. The discrepancy between the last two columns of the bottom table is due to the fact that the calculated attributes assume a perfect zigzag geometry, however, the geometry of the actual pattern strays from being perfectly zigzag.

The impact of such distortions on the linearity of the pad response may be significant, we, therefore, measured the pad response by scanning the acceptance of a quadruple GEM equipped with the new zigzag PCB using a highly collimated beam of x-rays. The results are shown below in Figure 7. Overall the results look very promising despite the structural short-comings of the fabrication process. While the pad response for this board exhibits a pronounced differential non-linearity, as indicated by the excursions from a straight line with a slope of one in the third top plot from the left, this deviation is very predictable. That is, while the response is only piece-wise linear, simply multiplying the calculated position by a factor about 2.0 will restore uniform linearity. Also, while the global position resolution is in excess of 250µm, the same multiplicative operation results in a global position resolution of about 70µm. However, these calculations have all excluded single pad hits, of which there are many. As seen in the bottom, left-most plot, single pad hits are quite prevalent for this PCB (at least when using x-rays to generate the primary charge), therefore the fabricated PCB is still far from ideal.

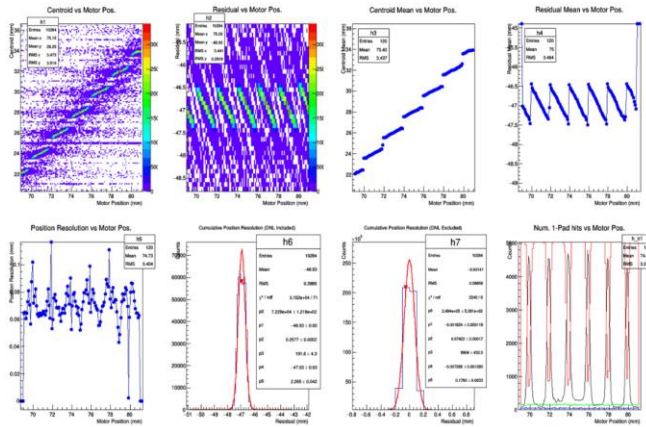


Figure 7 Suite of measurements from x-ray scan of zigzag PCB, including actual/measured position correlation, resolution vs position, the global position resolution, and the pad hit cluster size vs position. For the bottom left-most plot, the black curve corresponds to single pad hit cluster, blue: 2 pad hits, green: 3 pads hits, and blue: 4 pad hits.

Another interesting aspect of these results is that the error in the calculated position tends to pull the centroid away from pad centers and toward the center-line between pads. This contrasts with what one would expect if the simple geometry of the zigzag pattern drove the charge sharing. So, to better understand the detailed charge sharing characteristics of the zigzag structure, we have developed a very simple model that approximately reproduces the observed pad response. The model incorporates the linear response expected from the geometry of the zigzags alone, namely that charge division along the edge of the diagonal of a rectangle is directly proportional to the center of gravity of the deposited charge, as illustrated in Fig. 5. Secondly, and perhaps, more importantly, it also incorporates a weighting function which allows for the possibility for different regions of the zigzag to effectively collect an amount of charge disproportionate with respect to the area of that region. The concept behind this is that the directionality of electric field lines can disproportionately bring more charge towards the tips of the zigzag compared to other areas.

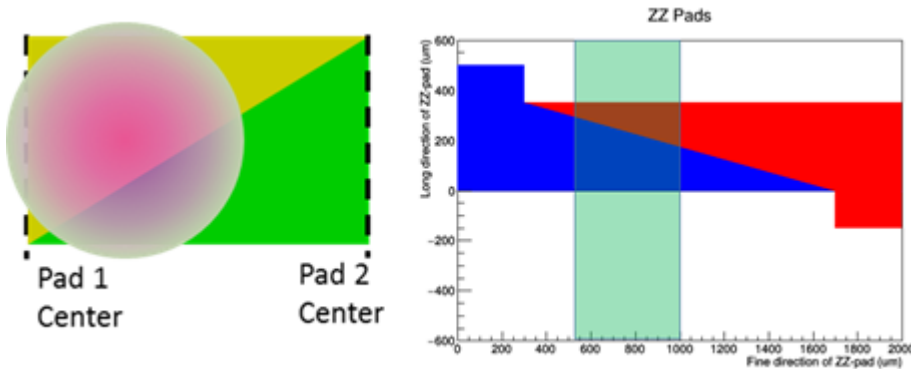


Figure 8 Left: An idealized sketch of the overlapping region of neighboring zigzag pads, with zero space gap between them, conceptually reveals the linear relationship between charge division and hit position. Right: Overlapping region of neighboring pads modeled in a simulation that uses the boundaries of the green rectangle (representative of the size of the charge cloud footprint on the readout plane) to allocate charge to each pad based on the bounded area. (The columns at the center of each pad at 0 and 2000 μm , represent single pad hit regions.)

To make the model as realistic as possible, it attempts to emulate the distortions seen in the manufactured zigzag electrodes described above. Most notably, the model allows for the zigzag tips to be eroded by a given amount to mimic the over-etching observed. This is done in such a way to preserve the zigzag angle, and thus the slope of the diagonal in the sketches in Figure 8, as was observed in the PCB described above. Also, since over-etching results in less overlap between neighboring pads, the degree of tip erosion defines the area over which there is no pad overlap, which can potentially result in single pad hits.

As discussed above, while the pad geometry is relatively accurate within the model, this alone cannot account for the observed pad response. So, in addition to geometry, we included a multiplicative weighting function which serves to emphasize and/or de-emphasize the impact of some regions over others. For simplicity, we applied a linear weighting function to emphasize the impact on the centroid calculation at the zigzag tips and to de-emphasize the impact at the pad center. The plots in Figure 9 illustrate how this is done.

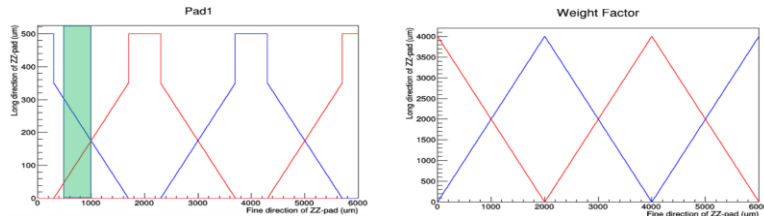


Figure 9 Left: the red and blue curves represent neighboring zigzag pad boundaries, so the area under each curve in the green box (ie the charge cloud) represents the collected charge, under the naïve assumption that pad area is proportional to charge. Right: the red and blue curves represent linear weighting functions used to multiply the instantaneous area in the centroid calculation.

The plots in Figure 10 compare the results of the model to the measured results. As long as accurate zigzag parameters, including the pitch, period, zigzag angle, the degree of tip erosion, and a charge cloud with an extent between 300-400 μm are used in conjunction with a linear weighting function as described, the resultant curve from the simulation is similar to the measured results. Both plots are quasi-linear, with the same slope, and while single pad hits were removed from the measured plot, they are apparent in the simulation results as short, discontinuous horizontal lines.

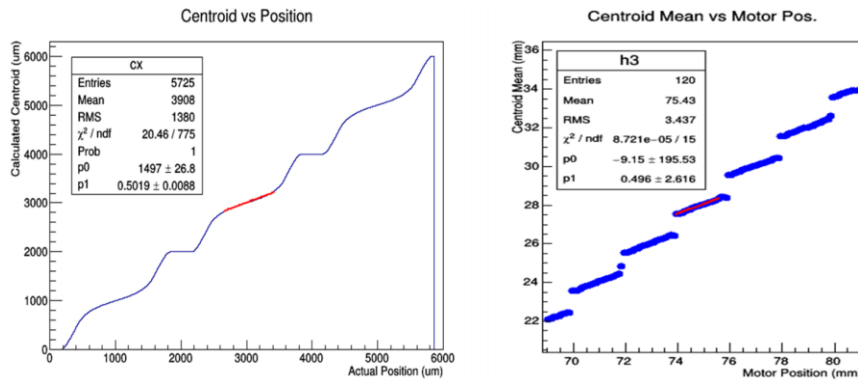


Figure 10 Left: position vs centroid calculation from simulation. Right: position vs centroid calculation from x-ray scan measurement. Both plots show a piece-wise linear response with a slope of about 0.5.

2. GEM Studies

Additional GEM studies were carried out to test the stability and energy resolution of a quadruple GEM filled with a new gas under consideration, Ne/CF₄ (90/10) due to its favorable transverse diffusion in a future TPC. Figure 11 shows the gain curve using this gas mixture, compared to other gas mixtures used in the past. Also, an energy resolution of about 8.4% was obtained with this gas, as shown in the plot to the right.

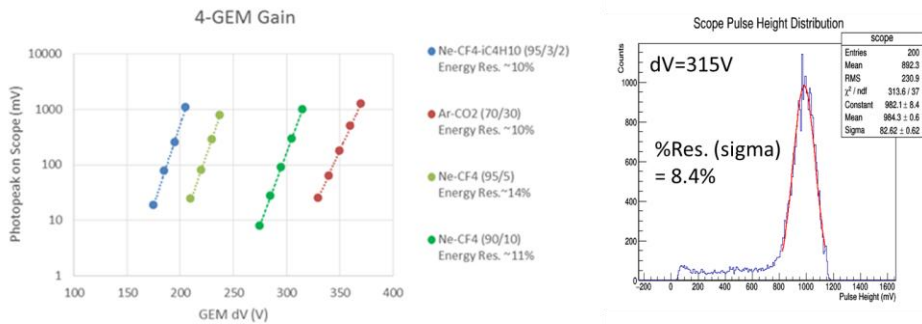


Figure 11 Gain curves and energy resolution of TPC gases under consideration.

Overall, Ne/CF₄ (90/10) exhibited very stable operation with no significant amount of sparking in the 4-GEM after a full day of operation.

1. Construction of next full-size EIC Forward Tracker GEM detector prototype. The three currently proposed EIC detector designs (BeAST, ePHENIX, JLAB IP1 central detector) feature virtually identical conceptual designs for the forward and backward tracking regions. In all three detector designs, both regions are instrumented with multi-layer tracker disks made from large-area GEM detector modules that provide acceptance from close to the beam pipe out to a radius of almost one meter (Figure 12) The forward tracking group (Florida Tech, U. of Virginia) of the eRD6 consortium has been conducting R&D that targets the development of affordable low-mass GEM detectors for this common subdetector system. Florida Tech is currently constructing a prototype of a 30.1° large-area GEM FT module for such a forward tracker GEM disk (Figure 13).

The leakage currents of four common FT GEM foils (Figure 14, Figure 16) designed at Florida Tech and produced at CERN were tested under HV in dry nitrogen and all were found to be acceptable. Figure 15 shows the leakage current for one foil as a function of HV while running a ramping profile for the HV. A fifth foil that has macroscopic production defects and is not suitable for a detector was recently sent to Temple U. for use in the commissioning of their new microscope scanning

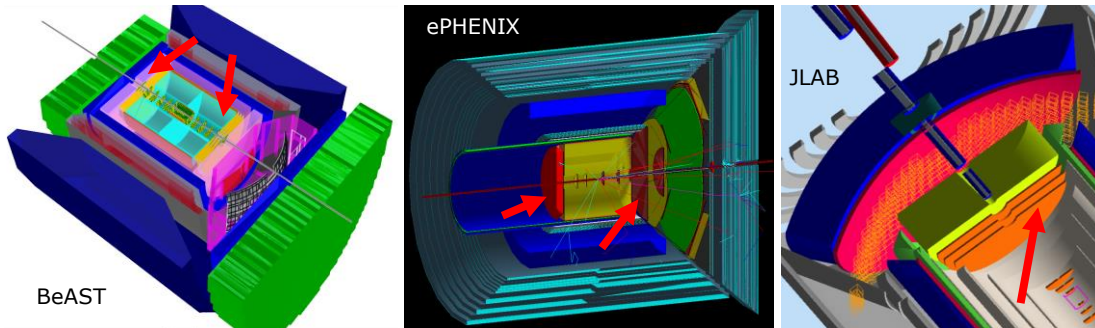


Figure 12 Commonality of the design of the forward and backward tracking regions with GEM detector disks (red arrows) in the currently proposed EIC detectors.

station for large GEM foils.

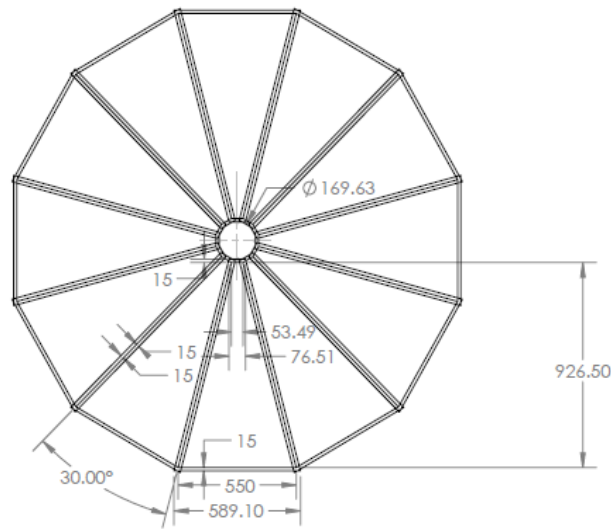


Figure 13 Conceptual design of a forward tracker GEM disk for an EIC detector.



Figure 14 Four large-area common EIC GEM foils for forward tracker under test in the cleanroom at Florida Tech.

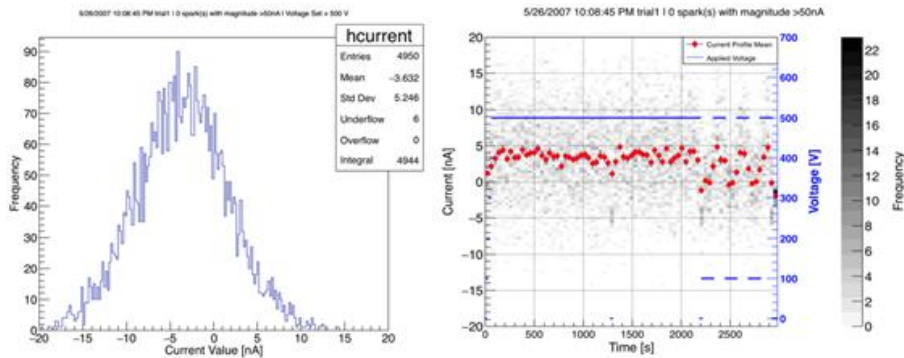


Figure 15 Left: Leakage current for one of the EIC GEM foils at 500V in dry N₂. Right: Leakage current measured while ramping HV (blue) through a test profile. Gray points represent the full data set and red points are mean values.

The new prototype achieves low mass by replacing the solid drift and readout PCBs of the first large prototype by flex-circuits on foils. The 1-meter-long zigzag readout foil for the prototype that had been designed at Florida Tech was received from CERN (Figure 16, Figure 17). Inspection of the zigzag structure under a microscope (Figure 18) shows a high-quality zigzag structure with good interleaving of zigs and zags similar to the 10 cm × 10 cm test foil that was successfully tested



Figure 16 Left: Readout-strip side of FT readout foil. Connectors for front-end readout electronics are visible at wide end of the trapezoid. Right: Zoom of inner radius sectors of foil that show transition from radial straight strips in innermost sector to radial zigzag strips in all other sectors. with X-ray scans at BNL previously and produced spatial resolutions well below 100 μm (see Jan 2017 report).

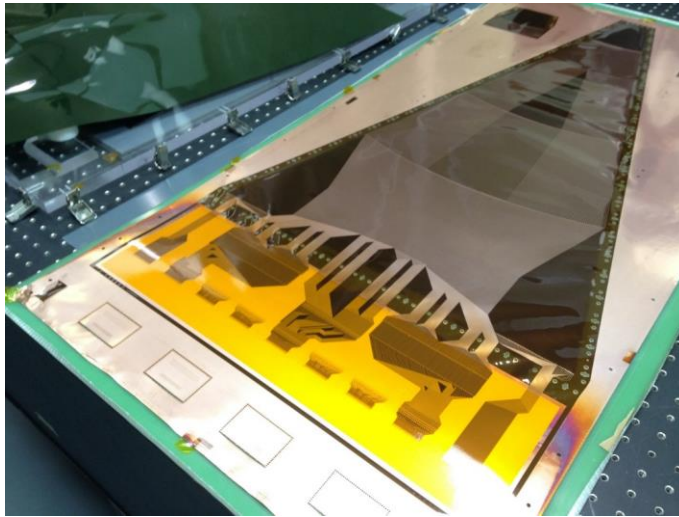


Figure 17 Signal-trace side of large FT readout foil.

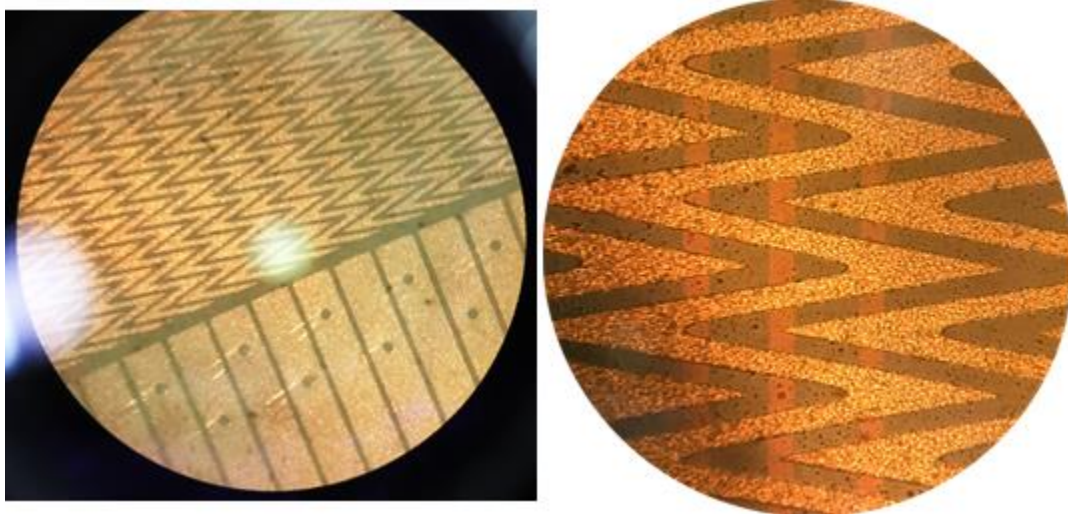


Figure 18 Microscopy photos of zigzag readout strip structures of large FT readout foil. Left: Transition region from radial straight strips in the innermost sector to radial zigzag strips in all other sectors. Notice that both structures have the same angular strip pitch. Right: Zoom of zigzag structure that shows sharp points and good interleaving of zigs and zags. The faint vertical strips are signal traces running on the back of the foil.

Our undergraduates Matt Bomberger and Francisco Izquierdo have manufactured the outer carbon fiber frames (Figure 19) that will hold the tensioned foils. The frames are a composite of eight layers of intermediate-modulus uni-directional carbon fiber (“IM7”) and Araldite epoxy (AY103). Each of the two frames is about 4 mm thick. Preliminary tests show that the frames structure should buckle-less than 1 mm when under full tension load from the five foils.



Figure 19 Carbon fiber frames manufactured in-house by undergraduate students under first tension test.

2. Publication of results from the X-ray studies of 10 cm × 10 cm zigzag boards

A manuscript describing results on the performance of improved zigzag structures presented in our Jan 2017 report has completed internal review by the authors from Florida Tech and BNL. We expect to submit it to NIM A before the EIC R&D review meeting in July 2017.

INFN Trieste

Activity in period October 2016-June 2017

Two R&D items were foreseen for the FY 2017, namely:

1. the test of **novel materials for the THGEM PCB** to simplify the detector construction, increase the production yield of large-size THGEMs and, thus, simplify the detector construction and control the detector costs;
2. the **development of resistive MM by discrete elements with miniaturized pad size** (present size: 8 x 8 mm²) in order to obtain finer space resolution, required to cope with the modest lever arm related to the limited radiator length; this activity is planned to start in Spring 2017 and to continue during the year 2018.

The two activity items have been fully financed for the FY 2017. Unfortunately, the administrative aspects of money transfer to INFN have not yet been completely worked out and the financial support is, in practice, not yet available. Nevertheless, so far, the activity has suffered only of a very marginal delay thanks to:

- INFN matching funds (13 k euro) granted in February 2017: these resources have been mainly used to support the needs of item 1;
- Item 2 is in design phase and has not required, so far, important financial resources;
- Two postdocs supported one within the AIDA-2020 project (European Union's Horizon 2020 research project and innovation program under the Grant Agreement No. 654198) and the other one by INFN offer a part-time contributor to these activities.

1. *test of novel materials for THGEM substrate*

THGEMs by PERMAGLAS have been produced and fully characterized; the main outcomes are reported in the following; **THGEMs by ARLON® 25 FR** (an epoxy laminate woven fiberglass reinforced, ceramic-filled composites using a non-polar, low loss, thermoset resin) have been produced and the characterization studies are presently starting.

Permaglas ME730 by RESARM Engineering Plastics SA (RESARM Engineering Plastics SA, rue Près-champs 21, 4671, Barchon, Belgium) is an epoxy glass fiber material, amorphous (no fiber weaving) and, therefore, easily machinable. The material components are the same as for fiberglass, nevertheless, the material structure is substantially different and it is expected that the smoother internal surface of the holes contributes in providing a good electrical stability of THGEMs by Permaglas. The planarity of Permaglas plates is obtained by machining.

We have purchased samples of Permaglas plates, 50 x 50 cm², of two different nominal thicknesses: 0.70 mm (nominal tolerance: -0, +0.05 mm) and 1.00 mm (nominal tolerance: -0.04 mm, +0.04 mm). The thickness uniformity is a key requirement for the THGEM performance: in fact, the gain uniformity of a THGEM is strongly related to the thickness one. It is expected that the plates with a nominal thickness of 1.00 mm are more uniform because this is the standard production thickness while machining obtains thinner plates. The thickness of the Permaglas plates has been measured in a grid of nine points uniformly distributed on the plate surface. The peak to peak thickness variation is 4% and the r.m.s. is 2% for the plates with a nominal thickness of 0.07 mm, while these parameters are, respectively, 2% and 1% for the 1.00 mm plates. These figures are very promising.

THGEMs have been produced with the following geometrical parameters: hole diameter of 0.4 mm, hole pitch of 0.8 mm, no rim. GEMs of both thicknesses have been produced. The size of the active area is 30 x 30 cm², segmented in 6 strips electrically independent. In the following, we report in detail on the characterization of THGEMs with a nominal thickness of 1.00 mm.

The electrical stability of the THGEMs is studied by the Paschen test, namely comparing the maximum voltage that can be applied between the two THGEM faces with the phenomenological Paschen limit that provides the maximum voltage that can be applied between two electrodes in a given atmosphere composition, at given pressure and temperature. A good THGEM should reach at least the 90% of the Paschen limit. Increasing voltage is applied to each of the six individual segment strips of a THGEM under controlled atmosphere, pressure and temperature; typically, not all the segments immediately reach the maximum voltage: in fact, the voltage application also acts as a commissioning procedure. The final voltage reaches or overcomes 90% of the Paschen limit for all the sectors of the studied Permaglas THGEMs, as shown in the example presented in Figure 20. Therefore, it is concluded that the THGEMs by Permaglas exhibit good properties of electrical stability.

The characterization studies have been performed with the Permaglas THGEMs in single layer arrangement (Figure 21)

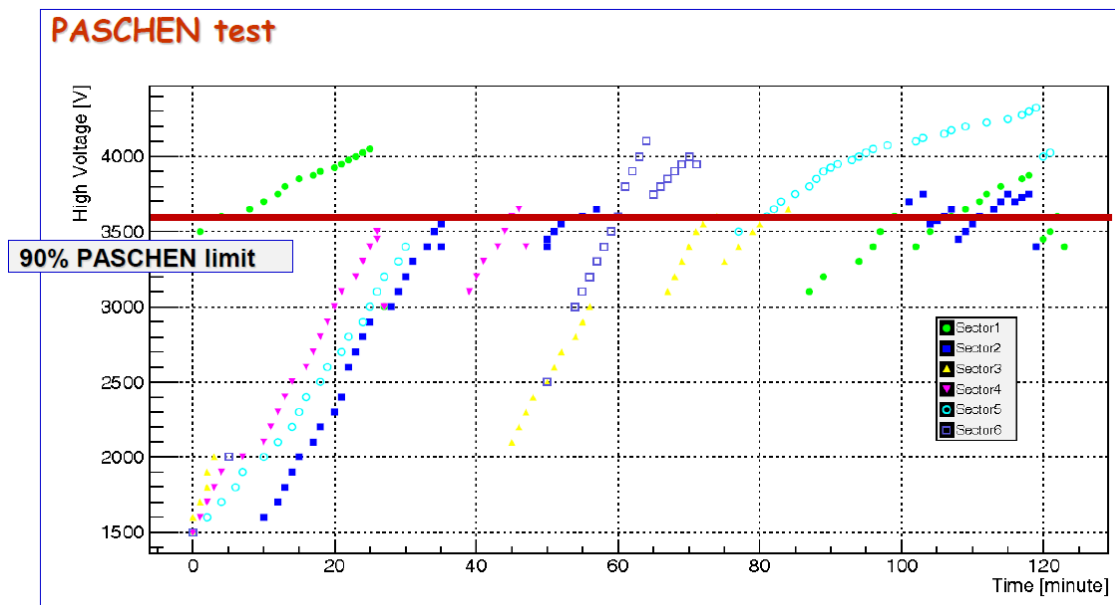


Figure 20 The results of the Paschen test for the six segments of a 1.00 mm thick THGEM: the applied voltage versus the time is shown.

using a gas mixture Ar:CO₂ (70:30) and a ⁵⁵Fe source.

Figure 22 presents a typical amplitude spectrum; the resulting resolution is r.m.s. 20%. The gain uniformity has been measured collecting spectra in a grid of 18 points (Table 1): the r.m.s. of the distribution of the 18 gain measurements is 13%. The gain evolution versus the applied voltage is shown in Figure 23: the expected exponential behavior is verified and

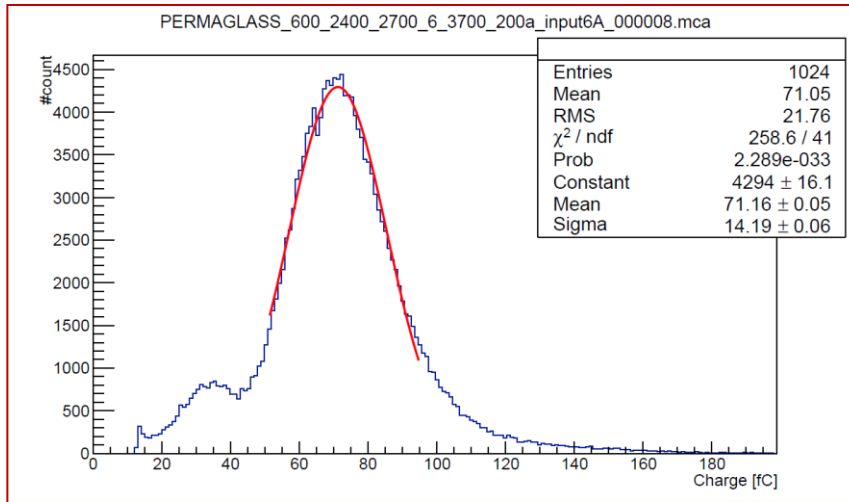


Figure 22 Amplitude spectrum obtained illuminating a Permaglas THGEM is single layer configuration with a ^{55}Fe source.

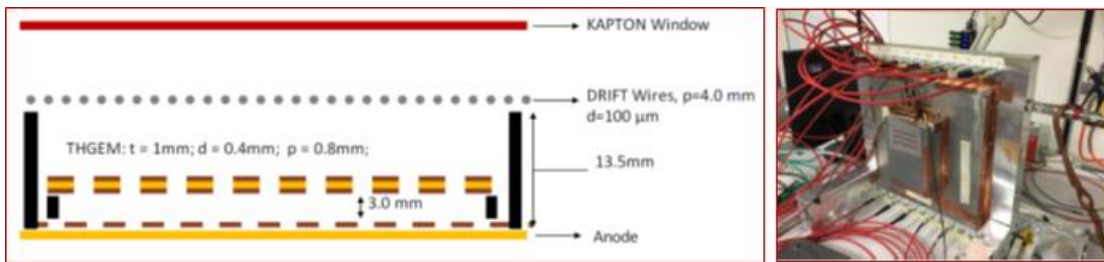


Figure 21 (Left) Schema of the single layer Permaglas THGEM detector used for the characterization studies; (Right) detector picture.

the detector is electrically stable up to relevant gain values, larger than 500. The gain studies show typical THGEM resolution in amplitude measurement, remarkably good gain uniformity and high gain potentialities.

Effective gain	1	2	3	4	5	6
A	150	139	139	134	120	121
B	121	108	101	103	116	116
C	142	105	121	121	116	90

Table 1 The gain uniformity measurement: the values of the main amplitude spectrum obtained illuminating with a ^{55}Fe source are reported.

The gain evolution versus time of a THGEM has two components: (i) one, faster, due to the charging up of the open dielectric surfaces and a second one (ii), slower, related to the motion of ions in the biased dielectric material. Both effects have been

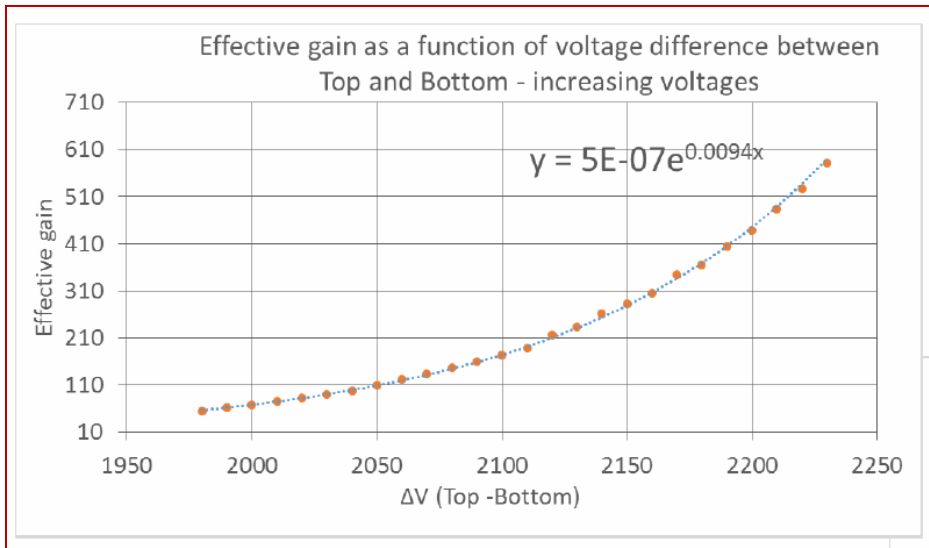


Figure 23 Effective gain of the single layer Permaglas THGEM versus the THGEM biasing voltage.

studied.

i. The gain evolution due to charging up is shown in Figure 24: it is described by an exponential function with a time constant of about 23 minutes and maximum gain excursion of the order of 30-40%. Both time constant and gain excursion depend on the illumination rate. The behavior observed is typical for THGEM multipliers.

ii. The gain evolution due to the motion of ions is illustrated in Figure 25: it is described by an exponential function with a time constant of about 333 minutes and maximum gain excursion of the order of 20%. The relatively short time constant and the modest gain excursion qualifies Permaglas as a very good material for THGEM production. In fact, in THGEMs by fiberglass, gain excursions up to 500% and time constants of the order of 1 day have been reported.

In conclusion, the characterization studies qualify Permaglas as a suitable material to produce high-quality THGEMs. In particular, the gain uniformity, the high gain achievable preserving electrical stability and the modest gain evolution versus time due to the internal ion motion in the biased material exhibit remarkable good features suggesting the use of Permaglas in applications for fundamental science.

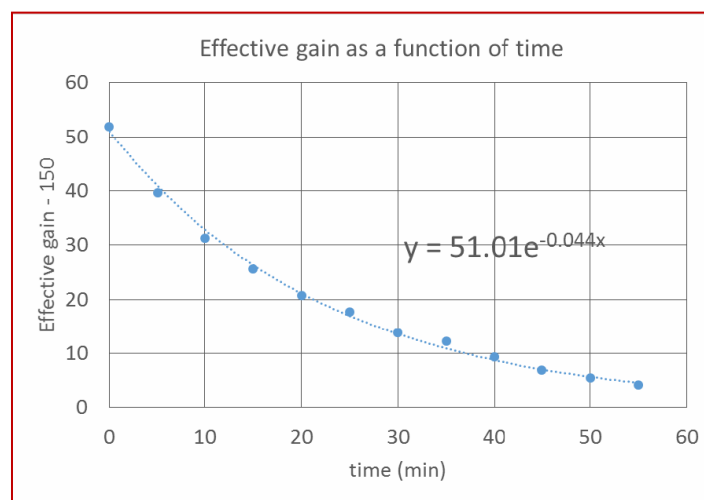


Figure 24 Gain evolution of a single layer detector including a Permaglas THGEM versus time: charging up effect.

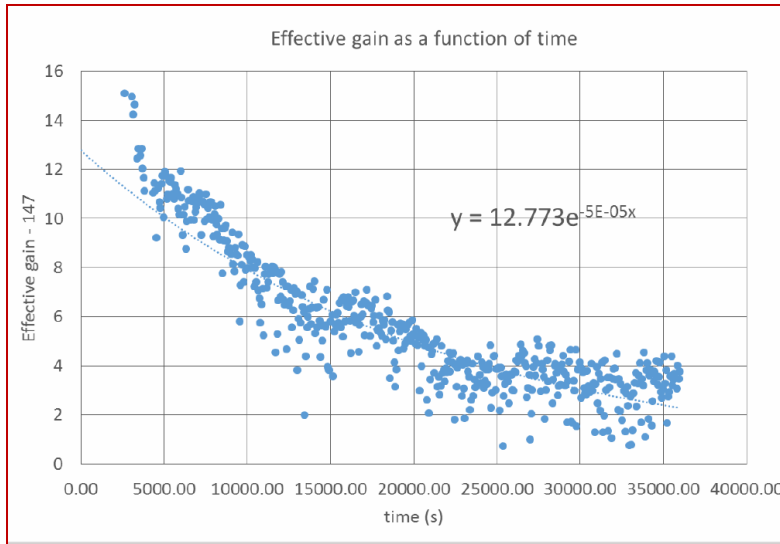


Figure 25 Gain evolution of a single layer detector including a Permaglas THGEM versus time: ion motion effect.

2. *development of resistive MM by discrete elements with miniaturized pad-size*

A detector prototype is being designed with the goal of reducing the pad-size from the present size, namely $8 \times 8 \text{ mm}^2$, to the reduced size of $3 \times 3 \text{ mm}^2$, with 3.5 mm pitch. The prototype active area is $10 \times 10 \text{ cm}^2$. One of the main design criteria is the easy expandability of the active surface. For this purpose, all the detector services, namely the read-out FE cards and the boards carrying the resistors in series with each pad, are included in an area not exceeding the active surface; the design is modular and based on groups of 128 pads (32×4). A key parameter is the selection of a commercial, robust connector coping with the available surface and the number of contacts required (two per pad: a resistor for the HV line and signal): the selected connector is SAMTEC, FTE series.

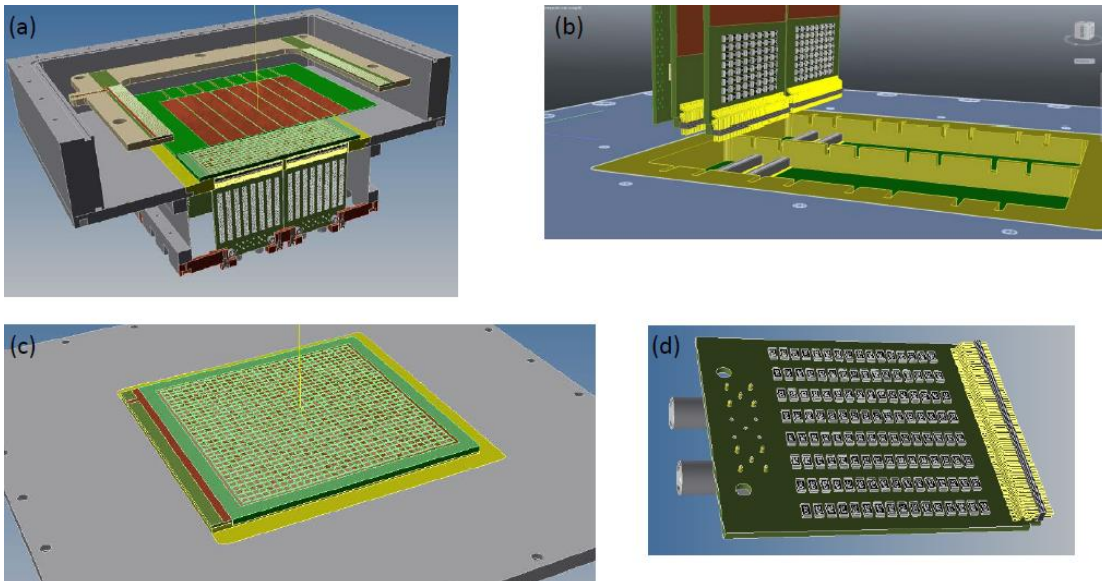


Figure 26 The design of the prototype of the resistive MM by discrete elements with miniaturized pad-size. (a) The overall detector. (b) The rear side: all the detector services are included within the active area. (c) The internal face of the anode: the pads are visible. (d) The board hosting 128 resistors to supply the HV to a corresponding number of pads.

The overall design is illustrated in Figure 26. The layout of the anode PCB, that hosts the pads and has to ensure the connections between pads, resistors and FE cards is in progress. A company able to guarantee a satisfactory realization of this complex and delicate PCB has been identified.

In parallel, the read-out system to study the prototype is been prepared; it is based on the SRS (Scalable Read-out System) with APV25 FE chips. The activity concerns the refurbishing of the available DAQ software and its enrichment with diagnostic and monitoring tools. An existing MPGD prototype is used to debug and test the improved DAQ system (Figure 27).

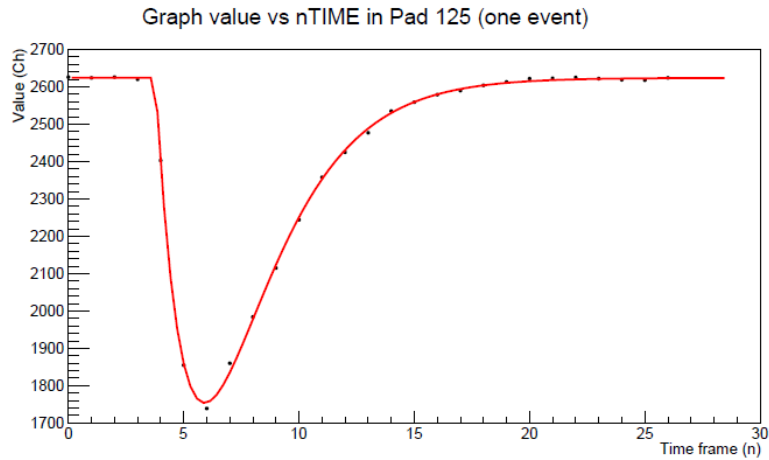


Figure 27 Signal collected using the refurbished DAQ system.

Stony Brook University:



Figure 28 Evaporator in the clean room of SBU. Left: side view. Right; View inside the evaporator.

All needed equipment had been identified, purchased, and received by the time of this write-up. We obtained 50 mirror blanks of lightweight carbon fiber reinforced polymer. These will be placed in strategic positions on a frame that resembles a typical large mirror blank. We also obtained a commercially produced mirror with certified reflectance which will serve as an absolute calibration device.

The evaporation equipment is being prepared to be installed into the evaporator (Figure 28). After installation, we must gain experience to perform the evaporation process. We have the support of an experienced specialist at Stony Brook University to perform the installation and the start-up of the evaporation system. He also guided us through the process of obtaining the proper equipment.

Univ. of Virginia

R&D on Chromium GEM (Cr-GEM):

1. Setup for aging study of Cr-GEM in X-ray test box

We received a new batch of three Cr-GEM foils from CERN earlier this year (2017). After optical inspection and electrical current leakage test were performed as standard quality control we replaced the damaged foil in the Cr-GEM prototype by one of the new Cr-GEM and put the chamber in the x-ray setup at UVa for a two-month-long aging test

study. Figure 29 shows the setup with two small prototypes, the Cr-GEM prototype with Chromium GEM foils and std-GEM with Copper GEM foils in the x-ray box. The std-GEM, which actually is the small EIC-GEM prototype with U-V strips readout is used as reference to compare aging performance of Cr-GEM and standard GEM foils. The std-GEM chamber is also used to correct for the gain variation as function of the pressure and temperature as will be shown in the following sections. The different strip readout layers, 2D U-V strips for std-GEM and is 2D X-Y Cartesian for the Cr-GEM is irrelevant for the aging studies.

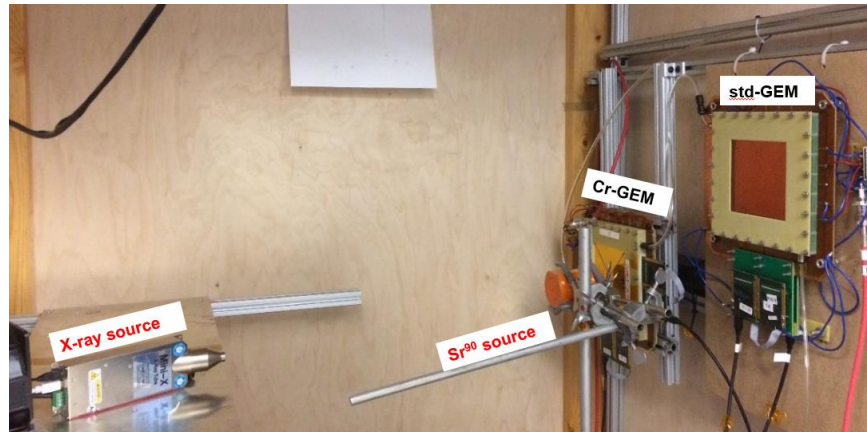


Figure 29 Cr-GEM prototype (Cr-GEM foils) and std GEM prototype (Cu-GEM foils) in the x-ray test box for aging test. Sr90 source is also used during the aging test

The setup also includes a Sr90 source as seen on Figure 29. Figure 29 Cr-GEM prototype (Cr-GEM foils) and std GEM prototype (Cu-GEM foils) in the x-ray test box for aging test. Sr90 source is also used during the aging test, used to test the basic properties of the chambers. Figure 30 shows the gain (left) and efficiency (right) curves from voltage scan performed on Cr-GEM prototype at the beginning of the aging test. The gain curve shows the expected exponential rise as a function of the HV and efficiency of 95% was achieved at the plateau at 4100V which is typical for a triple-GEM. These two results indicated that Cr-GEM foil displays similar gain performances to standard foils.

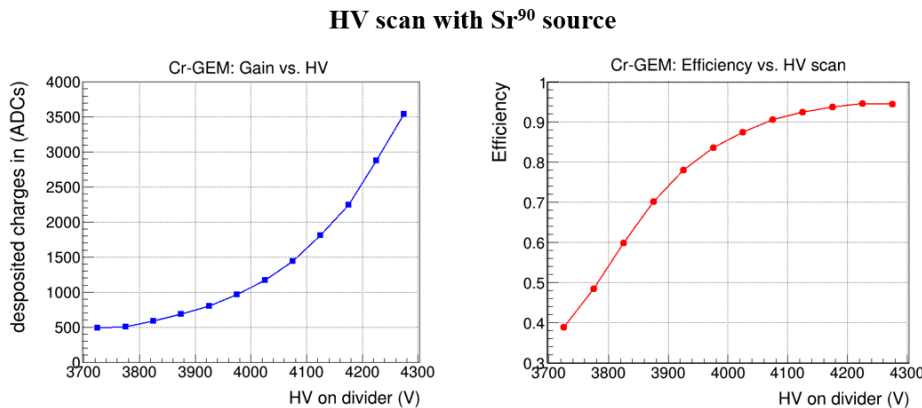


Figure 30 HV scan for gain and efficiency curves with Sr⁹⁰ at the start of the aging test run.

With the x-ray photon producing on average more than 10 times more primary than a m.i.p. particle, operating a triple GEM in a x-ray source at a gain equal 1000 is equivalent to operating the chamber at a gain of 10^4 for minimum ionizing particle m.i.p. for which this type of detectors is designed for. **Therefore, in the remaining sections of the report, when we refer to low gain (~1000) with x-ray source, but we should keep in mind that this is equivalent to operating at gain 10^4 in normal operating condition.**

2. Aging test results of Cr-GEM prototype:

The left plot of Figure 31 shows the stability of the gain as a function of time under continuous x-ray exposure. For this test, chambers were placed under continuous exposure to a moderate flux of the x-ray source. For the first 35 days, Cr-

GEM chamber was operating at voltage of 3800V corresponding to a gain of ~ 1000 . The std-GEM chamber operates at 3950V for a gain of approximately 3000 \sim 5000. From day 35 to day 65, we increase the voltage in Cr-GEM to 3950 in order to reach a higher gain of 5000. Data were acquired once a day to monitor the gain and study the performance of the chambers under irradiation. The plots show strong variation of the average gain for both detector but a good correlation of the gain change between the two chambers. This is an indication that external conditions such as atmospheric pressure and temperature variation are the causes of the gain variation.

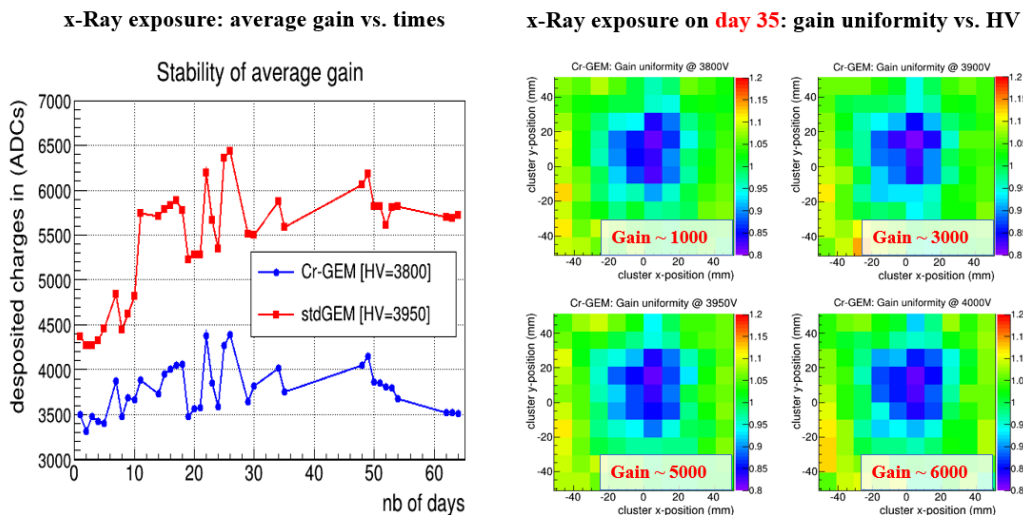


Figure 31 **Left**: Stability of the average gain for Cr-GEM and std-GEM as a function of continuous x-ray exposure time. The variation is due to temperature and pressure variation; **right**: Stability of gain uniformity of Cr-GEM for different HV (different gains in the chamber).

The right plot of Figure 31 shows the relative gain uniformity map for 4 different gains from 1000 to 6000. The gain uniformity remains stable at different gain but with a relatively large spatial variation which is likely due to non-uniformity of the holes distribution of Cr-GEM foils delivered by CERN.

As we can see on Figure 32, at a low gain of 1000, the estimated total daily charge seen by the Cr-GEM chamber is 4 mC over 10 cm \times 10 cm area. The chamber performance remains stable under continuous irradiation for 35 days which corresponds to average accumulated charges 1.5 mC / cm² on the chamber. We did not observe any damage, degradation or change of the average gain and of the gain uniformity as shown on the gain map plots on the left plot of Figure 32. The average gain remains stable with time after we corrected the gain variation caused by pressure and temperature by normalizing to the average gain std-GEM as shown on the right plot of Figure 32.

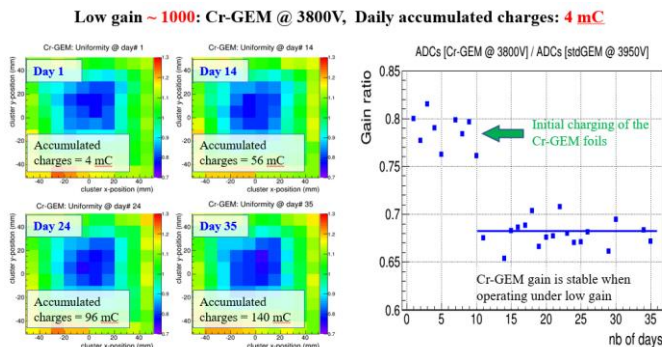


Figure 32 **Low gain condition**: Stability of the Cr-GEM gain under x-ray irradiation as a function of time at a gain of 1000. **Left**: spatial uniformity of the gain is stable over 35 days; **right**: The average gain ratio of Cr-GEM over std-GEM is stable with time.

After the month-long of irradiation with the chamber operating at low gain, we increases the HV on the Cr-GEM from 3800V to 3950V, which correspond to an increase of the gain from ~ 1000 to ~ 5000 . We also increases the x-ray current from 50 μ A to 75 μ A. The combined effect of high gain and high x-ray flux leads to increase the daily accumulated charges from 4 mC to 30 mC. Figure 33 shows the impact on the performances and stability of the Cr-GEMs. After a few days of exposure to higher flux at higher gain, the chambers starts showing some degradation of the gain uniformity as

can be seen on the left plot of Figure 33 on day 47, 54, 64. The non uniformity of the spatial distribution of the gain increases drastically after just 10 days of irradiation and the area with lower gain expand with times. The right plot shows a steady but moderate drop of the gain ratio between Cr-GEM and std-GEM which indicates that the gain of the Cr-GEM is slowing decreasing with time. The degradation is consistent with our previous observation with the first prototype which was tested under extremely high rate and high gain conditions leading to the “evaporation” of the Cr-layer on the bottom electrode of the 3rd Cr-GEM foil as we reported in previous progress reports.

These preliminary results seems to indicate that Chromium GEM foil is stable and can safely operate under normal gain condition (1000 when operating with x-ray source which correspond to a gain 10^4 for mip). However at high gain (5000 when operating with x-ray or 5×10^4 for mip) we observe some degradation and instability with the chamber.

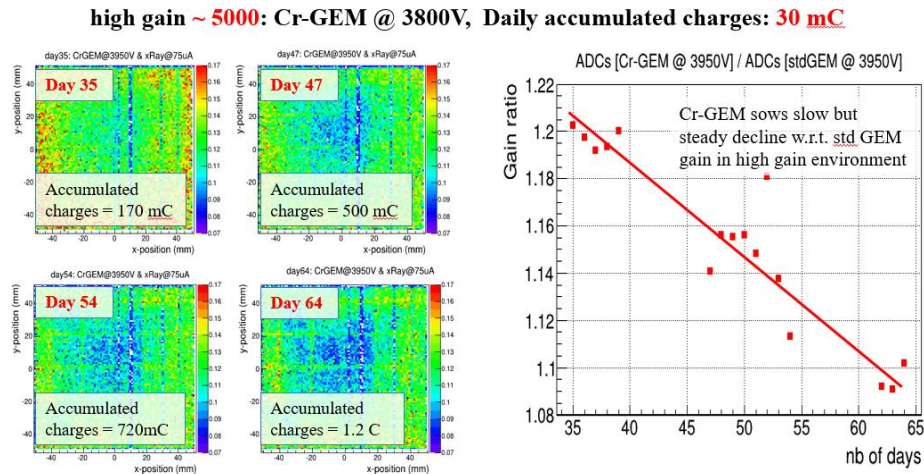


Figure 33 **High gain condition:** Stability of the Cr-GEM gain under x-ray irradiation as a function of time at a gain of 5000. **Left:** Degradation of the spatial uniformity of the gain, **right:** The average gain ratio of Cr-GEM over std-GEM show a slow but steady decline with time.

More study of the aging and stability of Cr-GEM detectors are needed to fully understand all the parameters that impact on the performances of this new technology and define the condition for a stable and reliable operation of Cr-GEM detectors.

Assembly and characterisation the large EIC GEM prototype II:

1. Validation of the Zebra connection concept on small prototype:

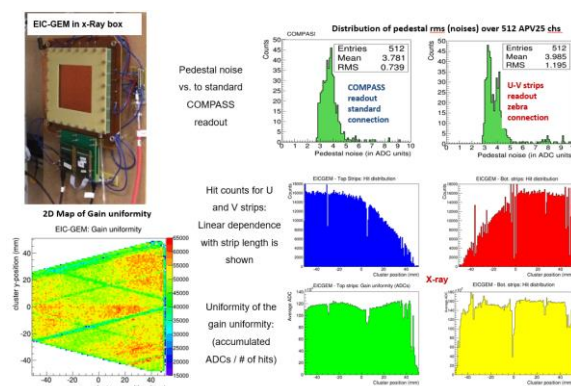


Figure 34 Test results of the zebra connection scheme with the small triple-GEM prototype with U-V strip readout in x-ray test bench.

As we already reported in the previous progress report, we have assembled a 10 cm × 10 cm triple GEM prototype with a small version of the U-V strips readout that is been developed for the EIC-FT GEM prototype. The small EIC-GEM prototype is aimed at testing some of the idea that we intend to implement on the full size prototype. One of the features we wanted to try out is the mechanical structure of the zebra connection scheme and the electrical properties of the connection. The details of the small readout and the zebra connection technique have been detailed in previous reports. On this document, we report the results from test and validation of the zebra connection scheme on the small prototype with x-ray source. Figure 34 shows the most meaningful results from the x-ray tests. The plots on the top-right shows comparable pedestal noise level of the U-V strips connected the APV25 FE cards through zebra connection with the noise level for standard COMPASS X-Y strips with similar strip length and standard Panasonic connectors soldered on the readout board. These encouraging results demonstrated that we we should not expect any unespected issues with pedestal noises with the large size readout layer. Figure 34 also shows hit distribution in U and V strips which clearly shows that the strip density are proportional to the length of the strips leading to the linear drop of hit counts for the strips in U (blue plot) and V (red plot) direction. The green and yellow plots at the bottom show the average ADC for each strip which shows a very good overall gain uniformity in the chamber.

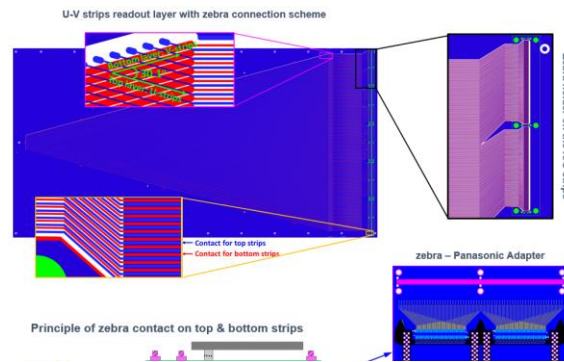


Figure 35 Design of the large U-V strip readout foil with zebra connection and the zebra-to-Panasonic adapter PCB for the full-size EIC-FT GEM prototype.

2. Production of full size U-V strip readout with the zebra kits

The main goal of tests of the small EIC-GEM prototype was to validate the zebra connection concept before the implementation on the large area for the full size EIC-FT GEM prototype. After the very positive and encouraging results, we finalize the design of the large U-V strips readout, taking into account the lessons learnt from the trial on the small prototype.

The drawings of the final design for the full size readout board with its zebra connection concept is shown on Figure 35. The production of the U-V strips readout foil and all elements of the zebra connection strips is under production at CERN PCB workshop

3. Low cost approach for the GEM chamber's support frames.

The design and production of the GEM support frames was put in hold last cycle due to lack of funding. Part of the additional support funding that we received earlier this year will be used for the frames. However, we would still need some additional in-house funding to be able to complete the production. In order to mitigate the high cost, we developed a new frame design that considerably reduces the cost of material and production. In the new design, the frame is made from 4 individual pieces (left picture of Figure 36) cut out of standard G10 material (material cost saving) that are later glued together into a frame in our detector lab. Using individual pieces, we allow us to cut all the pieces needed for 4 frames from one large raw G10 material to reduce even further material cost. The final assembly of frames at UVa save labour cost. However, only the 4 outer frames of the set of 8 frames of the EIC-FT GEM chamber can be produced based on this new approach. These 4 outer frames are the support frames for the entrance and exit gas window foils and are of directly part of the sensitive volume of the chamber.

Two sets of frames for the chambers to optimize cost and performances

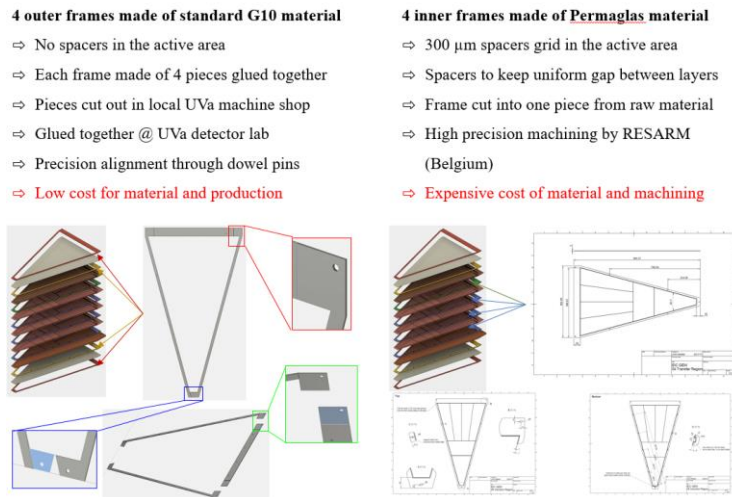


Figure 36 Set of frames EIC-FT GEM prototype. The 4 outer frames (left) are low cost material with less requirements. The 4 inner frames (right) are high quality material and high precision machining with higher production cost.

For the 4 inner frames that support the GEM foils and the drift cathode (right picture of Figure 36), we still need to use the special fiberglass material Permaglas as well as the fine precision machining of the 300 μm wide spacer grid inside the active area to maintain uniform gaps the detector. For these reasons, these frames are produced and procured from RESARM company from Belgium and the cost per frame is relatively high. We have finalized the two frames design and launch the production of the low-cost frames. We put in hold the production of the high cost frames for the moment while waiting for additional in-house funding to start the production

Yale University

1. Hybrid Gain Structure for TPC read-out – 2 GEMs plus Micromegas (2-GEMs + MMG).

More measurements were done with 2 new MMGs with resistive layer protection: TPC read-out style – Resistive strip was prepared for each TPC pad-row (production and delivery step from CERN micropattern detector workshop). Previous results which demonstrated a very low HV PS sensitivity to MMG sparking were confirmed - ~0.3 V drop for ~ 300 ms. For the hybrid setup gas amplification uniformity, energy resolution (⁵⁵Fe) and Ion Back Flow (IBF) were measured for Ar and Ne gas mixtures, and are in a good agreement with our previous data for the setup without resistive protection strips.

An ALICE IROC size 2 GEMs + MMG chamber without resistive protection was scanned using an X-ray gun (1“ steps in X and Y, and an ionization spot ~3 cm diameter) and demonstrated a low value and good uniformity for IBF (~0.25%) for gain ~2000 and energy resolution ~12% (⁵⁵Fe). Additionally, a stability test was done: 7 hours full detector X-rays illumination with > 10nA/cm² anode current.

No discharges were observed.

2. *Multi-element stacked gated grid.*

MWPCh plus three additional wire planes were prepared and tested to check that HV configurations can be found to get both options: high-efficiency electron transmission (open gate) and IBF practically zero (closed gate). The source of positive ions from gas amplification step with good timing parameters (fast start and stop) was established using UV-diode and Al cathode as a source of primary electrons.

We tested different options to prepare fast HV switches (-300 V to -600 V and -300 V to 0 V; with switching time smaller than 1 μ s).

What was not achieved, why not, and what will be done to correct?

Brookhaven National Lab

1. *Publication of TPCC results*

We postponed the submission of the paper on the beam test results of the TPC-Cherenkov detector in order to refine and add new analysis results. However, these tasks are now complete and a paper draft is in preparation where we plan to submit a manuscript to IEEE, TNS within the coming weeks.

2. *New high-intensity x-ray scanner*

The assembly of the x-ray scanner is essentially complete, however, the x-ray source was damaged during testing and had to be returned to the manufacturer for repair. We expect the x-ray source back within the coming weeks and will complete the commissioning process shortly after. We anticipate having the x-ray scanner fully operational this summer.

3. *GEM studies with Ne based mixtures*

Though we could measure the gain stability and energy resolution of some Ne-based gas mixtures, we were limited in what we could accomplish in this area mainly since there were no funds available to purchase an additional bottle of Ne gas, which is costly (\$5000.00 per bottle). In addition, we did not have the funds to purchase the correct mass flow controllers for mixing the gas components in the correct ratios, which very much limited our operation as well. Finally, we lacked the funds to purchase floating multi-channel pico-ammeters from PicoLogic (Zagreb, Croatia) which are necessary for performing the various GEM studies we are interested in, namely electron collection and extraction efficiencies vs ion back-flow rates in the TPC gas mixtures under consideration.

4. *FEE using SAMPA*

The SAMPA electronics prototype boards are not yet available to test. We anticipate that they will become available over the coming months.

Florida Tech

Completion of the procurement of all parts for the next FT GEM detector was delayed.

Local company Tru Mension Manufacturing Solutions (TMM Inc.) that was selected for producing the remaining mechanical components, such as halogen-free FR4 frames, pull-out posts, screws, etc. has incurred massive delays and become non-communicative. We are now looking for an alternative industrial source.

INFN Trieste

N/A.

Stony Brook University:

The final upgrade of the evaporator unit has not happened because the needed equipment did just arrive. We will be installing the system and will then start operating the evaporation system.

Univ. of Virginia

We did not perform the SEM inspection and the optical of the damaged Cr-GEM foil from the first prototype.

Procurement of the frames is on hold due to lack of funding. We are looking for some alternative source of funding to compete the production.

Yale University

We are still tuning the HV switches to achieve $\sim 1\mu\text{s}$ or less switching time. Currently, the switching time is $\sim 2\text{-}4\mu\text{s}$. In combination with pico-amperemeters, we will measure the crucial parameter: how fast positive ions can be collected in such multi-gate structure to compare with simulation results and measure how much dead time is required to achieve low IBF.

Future

What is planned for the next funding cycle and beyond? How, if at all, is this planning different from the original plan?

Brookhaven National Lab

We are planning to work on zigzag pad development, a GEM-based cosmic ray telescope and GEM studies using TPC gas mixtures in collaboration with SBU. The activities are described in the Proposals section.

Florida Tech

Our main goal for the next six months is to complete production of missing components for the new one-meter-long FT GEM detector with zigzag readout, assemble it, and put it through a battery of quality control (QC) tests modeled on the QC for the large GEM detectors of the CMS forward muon upgrade. This plan is unchanged.

INFN Trieste

In the coming year, we will (i) **continue and complete the two activity items started in FY2017** and we (ii) **propose to start a new strategic R&D item** related to gaseous photon detectors, that we illustrate in the following. Therefore, other R&D items originally proposed for next year, namely the comparison of THGEM vs GEM photocathodes in order to select the best architecture for gaseous photon detectors and further studies in order to enhance the IBF suppression in hybrid MPGDs, are postponed.

The novel activity proposed for next year concerns a **new photocathode based on NanoDiamond (ND) particles**: the planned activity consists in initial studies to understand the compatibility of this innovative photocathode material with the operation in gaseous detectors. **The possibility to use innovative photoconverters in gaseous detectors is a strategic option.** In fact, so far, the only photoconverter compatible with large-size, operative gaseous detector is CsI. Despite remarkable successful applications (for instance the read-out sensors of the ALICE RICH, the COMPASS RICH and the PHENIX HBD), the use of CsI in gaseous detector suffers from some intrinsic limitations: ageing, causing a severe decrease of the quantum efficiency after a collected charge of the order of some mC/cm^2 and long recovery time (about 1 day) after an occasional discharge in the detector. These limitations are related to the photon feedback from the multiplication region and to the bombardment of the CsI photocathode film by positive ions generated in the multiplication process. They impose to operate the detector at low gain, reducing the efficiency of single photoelectron detection. Alternatively, great care is required to reduce the IBF. Moreover, CsI is chemically fragile: if exposed, even for short time, to atmospheres with water vapor the molecule is broken and therefore the QE is lost. This feature imposes to assemble the photon detectors in clean, controlled atmospheres, making the overall detector construction tedious and complex. Therefore, the possibility of an alternative photocathode material adequate for gaseous detectors is strategic.

The Quantum Efficiency (QE) of photocathodes by ND particles rich in graphite have been measured in vacuum [L. Velardi, A. Valentini and G. Cicala, *Diamond & Related Materials* 76 (2017) 1]: when the photocathode is hydrogenized, QE as high as 47% at 140 nm has been measured; globally, the quantum efficiency is non-negligible in the VUV domain, below ~ 210 nm. High QE-values have been measured both performing the hydrogen plasma treatment in situ (after forming the photocathode film on the substrate) and hydrogenizing the ND powder before coating the substrate with the photo converting layer. The latter option is of great interest for gaseous photocathodes: in fact, the hydrogen plasma treatment requires high temperature ($< 800^\circ\text{C}$), not compatible with the components of gaseous detectors. When the ND powder is hydrogenized before the cathode coating, the spray procedure by an ultrasonic atomizer used to form the photocathode does not require temperatures exceeding 120°C : this is compatible with gaseous detector components. Preliminary tests of mechanical attachment of the photocathode and aging due to exposure to air indicate that this photocathode material is robust. Two principle difficulties must be considered in view of further studies [A. Valentini, private communication]:

- the ND powder provided by the producers is a cheap material not selected according to the graphite content; therefore, several different samples have to be purchased and then the graphite-rich ones have to be selected by Raman spectroscopy; no exact reproducibility of the raw material from producers can be envisaged;
- using the present set-up for the formation of photocathodes by the spray technique, the maximum photocathode size is of about 4 cm^2 .

For next year, we are planning a very basic set of studies:

- to compare the quantum efficiency of photocathode samples in vacuum and in different gaseous atmospheres;
- to realize a photon detector prototype with a photocathode using as substrate a THGEM and to characterize it;
- to perform a preliminary aging study measuring the QE before and after collecting defined amount of charge at the photocathode itself.

A colleague of the group who measured the hydrogenated ND QE and invented the spray technique will join the effort.

Concerning the **perspectives of all the future activities**, it should be remarked that:

- for the continuation and completion of the **on-going activities**, some delay is expected to be accumulated in the next months because of lack of resources as the granted financial support did not become effective: this is limiting the dedicated manpower and will prevent purchasing the components of the prototype of resistive MM by discrete elements with miniaturized pad-size; of course, we are at work to overcome administrative difficulties in order to make the financial support effective and limit the related delays; no new financial support specifically dedicated to these items is requested;
- for the **new proposed activity**, namely the preliminary studies towards a gaseous photon detector with CD photocathode, the newly required financial support is essential, both concerning material and manpower; a possible reduction of the financial support by 20% will definitely slow down the planned program, while a reduction of about 40% would oblige us to give-up on this strategic item.
- The expected timelines are shown in Table 2.

TASK no	TASK	FY 2017				FY 2018				FY 2019				> FY 2019			
		1st quarter	2nd quarter	3rd quarter	4th quarter	1st quarter	2nd quarter	3rd quarter	4th quarter	1st quarter	2nd quarter	3rd quarter	4th quarter	1st quarter	2nd quarter	3rd quarter	4th quarter
1	test of novel materials for THGEM substrate																
2	resistive MM by discrete elements with miniaturized pad size																
3	preliminary studies towards a gaseous photon detector with CD photocathode																
4	further studies towards a gaseous photon detector with CD photocathode, IF PRELIMINARY STUDIES PROMISING																
5	comparison of THGEM vs GEM photocathodes																
6	enhancement of the IFB suppression in hybrid MPGDs																
7	operation of hybrid MPGDs (THGEMs + MM) in fluorocarbon-rich gas mixtures																

Table 2 Timelines of the R&D activity. The new items are in color. Items 5,6,7 are postponed making the new strategic activity affordable.

Stony Brook University:

The finalization of redesigning the evaporator for producing large mirrors is expected to be performed in the Fall term of 2017. The equipment is being installed. We will be learning to properly operate the equipment and then provide a large surface equipped with smaller mirror blanks at each corner and in the center. The samples will then be evaluated with the VUV spectrometer from BNL. This should represent a good measure of the properties of a large mirror evaporation.

We propose to perform studies for a Time Projection Chamber to be used in an EIC detector.

Univ. of Virginia

For the next six months, our plan is to complete the assembly of the prototype after all the parts are produced and delivered as expected. The prototype will then be fully tested in cosmic and x-ray setup at UVa in preparation for the Beam Test at Fermilab. We are also planning to continue the aging test for the Cr-GEM chamber, exposing the chamber in moderate flux for a longer term (several months) at a moderate gain and monitor the aging performances.

Yale University

Our plan is to finish all R&D activities mentioned above and prepare at least 2 publications.

What are critical issues?

Brookhaven National Lab

1. Laser Etched zigzag PCB's

To further along the accuracy of fabrication for our zigzag PCB's we would like to purchase new zigzag PCB's fabricated using the laser etching process described above, which promises to deliver precision etching far superior to traditional chemical etching, at a reasonable cost.

2. *PicoLogic Pico-ammeters (Zagreb, Croatia)*

To perform the GEM studies described, we must purchase a set of compact pico-ammeters that can be floated to the high voltages applied to each GEM electrode. The pico-ammeters are fully programmable in terms of setting parameters like the integration time, and the number of averaged samples, etc., which are necessary features for our R&D program.

3. *New SRS + APV25 DAQ*

A new SRS + APV25 DAQ system is required for the new GEM based telescope we are planning to develop over the next few months. The telescope will comprise 4 layers of triple GEM detectors, each equipped with a 10x10cm² COMPASS X-Y strip readout containing 512 channels, in addition to about 512 channels needed for the detector under study. The SRS + APV25 system is ideal for such high channel applications in the lab.

Florida Tech

The departure of our post-doc Aiwu Zhang in Dec 2016 has severely slowed down progress. While our undergraduates have done a fine job and are very enthusiastic about building the new prototype detector, they have limited availability and experience.

We need to find another industrial source for procuring the missing detector components.

INFN Trieste

Stony Brook University:

We need to accomplish the evaporation process after a learning curve.

Univ. of Virginia

For this cycle, there is no critical issue other than the fact that we are still waiting for some additional in-house funding to complete the production of the GEM support frames in order to start the assembly of the chamber.

Yale University

Hybrid Gain Structure for TPC readout

Critical issues remain the same: develop methods for operating a TPC at high data rates while maintaining low ion feedback, good energy resolution and robust operation (low discharge rate).

Additional information: None.

Manpower

Include a list of the existing manpower and what approximate fraction each has spent

on the project. If students and/or postdocs were funded through the R&D, please state where they were located and who supervised their work.

Brookhaven National Lab

This work is being carried out by members of the BNL Physics Department. It includes one Senior Scientist (0.2 FTE), two Physics Associate (1.2 FTE), and one Technician (0.3 FTE). All personnel is paid by the BNL Physics Department.

Florida Tech

Marcus Hohlmann, P.I., 0.25 FTE, not funded under this R&D program.

Matthew Bomberger, physics undergraduate student, not funded

Francisco Izquierdo, mechanical engineering undergraduate student, not funded

INFN Trieste

Personnel involved in the project during the coming year:

TRIESTE

C. Chatterjee (Trieste University and INFN, PhD student)

S. Dalla Torre (INFN, Staff)

S. Dasgupta (INFN, postdoc)

S. Levorato (INFN, Staff)

F. Tassarotto (INFN, Staff)

Y. Zhao (INFN, postdoc)

1 new postdoc specifically enrolled for this R&D when the financial support will become effective; the postdoc will work under the supervision of S. Levorato and F. Tassarotto.

The contribution of technical personnel from INFN-Trieste is also foreseen according to needs.

BARI

Antonio Valentini (Bari University and INFN, professor)

Globally the dedicated manpower will be equivalent to 2.5 FTE.

Stony Brook University:

None of the labor at SBU is funded by EIC R&D. The workforce is

K. Dehmelt, Research Scientist, 0.4 FTE, T. K. Hemmick, Professor, 0.1 FTE, N. Nguyen, Undergraduate student, 0.25 FTE

Univ. of Virginia

None of the labor at UVa is funded by EIC R&D. The workforce is listed below (in % FTE):

N. Liyanage	Professor	0.1 FTE
K. Gnanvo	Research Scientist	0.4 FTE
H. Nguyen	Research Scientist	0.05 FTE
John Matter	Graduate Student	0.2 FTE

Yale University

None of the labor at Yale is funded by EIC R&D. The workforce is listed below.

R. Majka Senior Research Scientist and Scholar 0.1 FTE

N. Smirnov Research Scientist and Scholar 0.5 FTE

External Funding

Describe what external funding was obtained, if any. The report must clarify what has been accomplished with the EIC R&D funds and what came as a contribution from potential collaborators.

Brookhaven National Lab

Aside from supporting the personnel involved in this effort by the BNL Physics Department, we are not receiving any other funding from any other source. It should be noted that the sPHENIX Collaboration is developing a TPC for the sPHENIX experiment but our R&D on this project is not being supported by this effort.

Florida Tech

None.

INFN Trieste

A request for financial support from INFN will be placed for 2018: the outcome is expected by September 2017. The support level can be similar to the one received for 2017 (2017: €13k).

Stony Brook University:

There is no external funding for this R&D effort.

Univ. of Virginia

UVa has DOE basic research grant from Medium Energy Physics. The R&D work on Cr-GEM is funded with the research grant.

The group also has DOE grants through JLab for the construction of the SBS GEM.

Yale University

None.

Publications

Please provide a list of publications coming out of the R&D effort.

Brookhaven National Lab

A paper entitled “*Beam Test results from a Combination TPC-Cherenkov Detector*” is currently being prepared for submission to the IEEE journal, Transactions on Nuclear Science in the coming weeks.

1. “A Study of a Minidrift GEM Tracking Detector”, B. Azmoun [et.al.](#), IEEE Transactions on Nuclear Science, Vol. 63, No. 3 (2016) 1768-1776.
2. “A Prototype TPC/Cherenkov Detector with GEM Readout for Tracking and Particle Identification and its Potential Use at an Electron Ion Collider”, C. Woody [et.al.](#), proceedings of the 2015 Micropattern Gas Detector Conference, European Journal of Physics (in press).
3. “A Study of a Combination TPC-Cherenkov Detector using a CsI Photocathode and GEM Based Readout”, B. Azmoun [et.al.](#), in preparation for submission to the IEEE Transactions on Nuclear Science.

Florida Tech

1. Presentation: M. Hohlmann “A Large Low-mass GEM Detector with Zigzag Readout for Forward Tracking at EIC,” MPGD 2017 conf., Temple U., May 2017.
2. Manuscript in preparation: A. Zhang, M. Hohlmann, B. Azmoun, M. L. Purschke, C. Woody, “A GEM readout with radial zigzag strips and linear charge-sharing response,” to be submitted to Nucl. Inst. Meth. A; presented also as a poster at the 2016 IEEE NSS, Strasbourg, France.
3. Manuscript in preparation: M. Bomberger, A. Zhang, M. Hohlmann, “Mechanical design and stress analysis of a large-area gas electron multiplier,” in preparation for submission to Journal of Mechanical Design (JMD). This work was presented at the 2017 Florida Academy of Sciences annual meeting and received an “Honorable Mention Undergraduate Oral Presentation” award.
4. A. Zhang and M. Hohlmann, "Accuracy of the geometric-mean method for determining spatial resolutions of tracking detectors in the presence of multiple Coulomb scattering," JINST 11 P06012 (2016), June 21, 2016.
5. A. Zhang, V. Bhopatkar, M. Hohlmann, et al., "R&D on GEM Detectors for Forward Tracking at a Future Electron-Ion Collider", Proc. of IEEE Nuclear Science Symposium 2015, San Diego, CA; arXiv:1511.07913, Nov 24, 2015.
6. A. Zhang, et al., "Performance of a large-area GEM Detector read out with wide radial zigzag strips," Nucl. Inst. Meth. A 811 (2016) 30-41, online version at ScienceDirect (18 Dec 2015).

INFN Trieste

N/A

Stony Brook University:

1. M. Blatnik et al., “Performance of a Quintuple-GEM Based RICH Detector Prototype”, IEEE TRANSACTIONS ON NUCLEAR SCIENCE, VOL. 62, NO. 6, DECEMBER 2015.
2. M. Blatnik et al., “Performance of a Quintuple-GEM Based RICH Detector Prototype”, Nuclear Science Symposium Conference Record, 2015, IEEE
3. Manuscript in preparation: “First Results from a Prototype Combination TPC Cherenkov Detector with GEM Readout”, to be submitted to the IEEE Transaction on Nuclear Science in early 2017.
4. Proceedings in preparation: “First Results from a Prototype Combination TPC Cherenkov Detector with GEM Readout”, for the IEEE NSS/MIC 2016 in Strasbourg.

1. Presentation: K. Gnanvo “*Large GEM R&D for the Forward Tracking at the Electron Ion Collider*” MPGD2017 conf., Temple U., May 2017.
https://indico.cern.ch/event/581417/contributions/2556737/attachments/1463800/2262526/MPGD2017_GEM_TRD_KG_20170522.pdf
2. Presentation: K. Gnanvo “*Preliminary Results of GEM based Transition Radiation Detector/Tracker in Test Beam at JLab*”, MPGD2017 conf., Temple U., May 2017
https://indico.cern.ch/event/581417/contributions/2556718/attachments/1464747/2264079/MPGD2017_GEM_EIC_KG_20170523.pdf
3. K. Gnanvo et al., “*Performance in Test Beam of a Large-area and Light-weight GEM detector with 2D Stereo-Angle (U-V) Strip Readout*”, Nucl. Inst. and Meth. A808 (2016), pp. 83-92. DOI: [10.1016/j.nima.2015.11.071](https://doi.org/10.1016/j.nima.2015.11.071)
4. K. Gnanvo, et al. “*Large Size GEM for Super Bigbite Spectrometer (SBS) Polarimeter for Hall A 12 GeV program at JLab*”, Nucl. Inst. and Meth. A782, 77-86 (2015). DOI: [10.1016/j.nima.2015.02.017](https://doi.org/10.1016/j.nima.2015.02.017)
Yale University

Proposals

Brookhaven National Lab

Zigzag pad development

For the TPC to meet the physics goals of the EIC program, the performance criteria for the momentum resolution requires a single point track position resolution better than $200\mu\text{m}$. Considering the budget constraints on the channel count of the TPC readout, our strategy is to enhance the charge sharing of relatively large pads to such an extent that the single point position resolution is many times better than what the pad pitch would imply. The success of this strategy would then satisfy the resolution requirements within the imposed budget constraints.

We plan to continue the development and optimization of the zigzag pads, with a focus on pursuing more accurate fabrication methods. In particular, after speaking with several experts, we have learned that a laser etching process (PLCS) is available at reasonable cost, which seems to be among the most accurate fabrication techniques available on the market. Feature sizes down to about $25\mu\text{m}$ ($\sim 1\text{mil}$) are possible with this technique, far out-performing the specifications of traditional chemical etching. Thus, we would like to have new PCB's made using this process which provides smaller gaps between zigzag pads and increased pad overlap, for improved performance. However, we have not yet fully ruled out the use of high precision chemical etching to produce new PCB's, though this process comes at a premium in cost.

In parallel, we also plan to pursue more simulation work to fundamentally explain how the charge is shared among neighboring zigzag pads. The new simulations will include comprehensive electric field calculations to accurately model the transport of individual electrons from the induction gap to the collection electrodes.

GEM-based cosmic ray telescope

We plan to build a GEM-based cosmic ray telescope for the purpose of reconstructing cosmic tracks to high precision. These high precision tracks will be used as a reference to compare to tracks reconstructed using a sample detector, such as a minidrift GEM detector equipped with a zigzag PCB. This will provide an absolute measure of the position resolution for each PCB.

GEM Studies using TPC gas mixtures (collaborate with Stony Brook group)

We plan to continue doing GEM studies using gas mixtures favorable for a TPC, including gain measurements, energy resolution, and charge spread measurements when needed. However, we plan to focus more on studies to maximize electron extraction and collection efficiencies and reduce ion backflow by exploring the electric field ratios in neighboring gaps between GEMs, while maintaining adequate energy resolution.

Joint R&D Proposal from Florida Tech and UVa

For this FY18 funding cycle, Florida Tech and UVa are planning to conduct a joint test beam at Fermilab to test the performances of the two large forward tracker GEM prototypes that are currently being built at the two institutions. This will complete the baseline R&D project on large GEM detectors for the EIC forward tracker.

The two groups plan to slightly extend the joint R&D effort for the forward tracker with the development of large-area chromium GEM foils (Cr-GEM) and construction of a full-size triple-GEM detector to validate the encouraging results from the aging studies of Cr-GEMs performed on a small prototype at UVa with full-scale 1m-long GEM foils.

After completion of the forward tracker R&D program, the two groups plan to turn their attention to the development of a cylindrical fast tracker for the central region based on resistive microwell (μ -RWELL) detectors.

Beam Test of EIC-FT GEM prototypes at Fermilab (spring / summer 2018)

As described in the above sections of the eRD6 progress report, two full-size triple-GEM chamber prototypes are currently being built, one at Florida Tech with a zigzag strip readout and the second at UVa with a U-V strip readout. Though the assembly techniques and the readout structures are drastically different, the two prototypes share several common features. Both chambers use the common GEM foil design developed jointly by the two groups together with the eRD3 group at Temple University. Both groups are also making an effort to build very low mass detectors to reduce multiple scattering. We propose to test these new detectors at the Fermilab Test Beam Facility (FTBF) to study their performances such as spatial resolution, gain uniformity, and efficiency in a realistic charged-particle beam environment

in addition to test results performed with x-ray sources in our respective detector labs. The test beam data will provide a complete and comprehensive picture of the expected performances of these detectors in a final EIC forward tracker configuration. A tentative timescale for the test beam is a two-week period in spring or summer 2018 at Fermilab. We will take advantage of the organizational infrastructure of the FLYSUB collaboration that we had formed for the eRD6 beam test effort in 2013 and that is still in place at Fermilab. The results of the test beam will be subsequently presented at appropriate conferences and published in a peer-reviewed paper during the second half of the year 2018.

We request 10k\$ for travel to Fermilab including housing and per diem for two people per institution for a two-week beam test period plus \$3.5k for lab materials and consumables such as gas at Fermilab.

Development of large-area chromium GEM foil

Encouraging preliminary results of the aging test performed on the small GEM prototype using chromium GEM foils (Cr-GEMs) are presented in the UVa section of the eRD6 progress report. The UVa and Florida Tech groups will work together with the PCB workshop at CERN to develop a large-area Cr-GEM foil and test it on a full-size EIC FT GEM prototype.

a) Simulation of the impact of low mass Cr-GEM chambers on EIC tracking

We plan to perform a simulation of the impact of detector material budget and multiple scattering in the forward region of an EIC detector on the tracking performance to see how much Cr-GEMs will benefit the forward tracking performance. This will include the study of the matching of tracks to calorimeter clusters and using tracks as seeds for RICH ring reconstruction. A GEANT4 simulation package (eicroot) developed and maintained by Alexander Kiselev at BNL is available to perform this task. We are proposing to send two summer students (one from each institution) to BNL for a month in 2018 to get trained on the eicroot software package installation and utilization and to learn how to run the simulation with the help of A. Kiselev. The students will then simulate and analyze different detector material configurations. The simulation results will be subsequently presented at appropriate conferences and incorporated into a peer-reviewed paper during the second half of the year 2018.

b) Production of full-size prototype with Cr-GEMs

One of the crucial advantages of the purely mechanical GEM assembly technique used by Florida Tech for the EIC FT GEM prototype is that the chamber can be re-opened at any time which allows replacing or reusing any part of the detector. We are taking advantage of this feature to build a full-size triple-GEM prototype with Cr-GEMs at very low cost.

After completion of the test beam at Fermilab, the Florida Tech FT GEM prototype will be re-opened and two of the three standard GEM foils with 5 μm thick Cu will be replaced by new Cr-GEM foils produced at CERN. If funding for new Cr-GEM foils is not available, two existing GEM foils from the Florida Tech FT GEM prototype can alternatively be sent back to CERN to remove the copper and leave the 100 nm Cr layer. This second option of reprocessing existing standard GEM foils into Cr-GEM foils will reduce the cost by a factor of two, but carries a higher risk of losing a GEM foil since CERN cannot guarantee 100% yield on the copper removal process. For the EIC-FT GEM prototypes built at Florida Tech, the cost of 2 GEM foils is about 20% of the total cost of a full chamber as the cost of zigzag readout board as well as the R&D on the detector frames dominates. Consequently, the main aim of this part of our proposal is to build a full-size FT Cr-GEM chamber at very low cost by reusing most parts of the second Florida Tech prototype. The prototype will be assembled at Florida Tech with UVa participation and a cosmic test and an aging test will be performed at both UVa and Florida Tech. The detector will then be opened again to examine the state of the Cr-GEM foils after irradiation.

We request 4k\$ for two large Cr-GEM foils, 8k\$ for travel by two summer students to BNL, and 1.5k\$ for travel by Dr. K. Gnanvo to Florida Tech for the assembly and test of the large Cr-GEM prototype.

Development of cylindrical μ -RWELL detectors for acquiring fast hit information in the central EIC tracking detector

At the recent eRD3/6 tracking consortium meeting at Temple U. reported elsewhere in this document, the need for fast thin cylindrical detectors that surround the inner vertex detector and the TPC was identified and emphasized. Since the MAPS, which are currently slated for vertexing and inner tracking, integrate signals over significant time intervals and since the TPC has long drift times before signals arrive at the readout, a complementary detector is needed in the central region that

can provide fast hit information on a time scale of a few nanoseconds and with high spatial granularity. By linking this fast hit information to the continuously and more slowly acquired tracks in MAPS and TPC, the correct bunch crossing can be identified to allow proper event building in the tracking system.

We would like to propose micro-Resistive WELL (μ -RWELL) [1] detectors in cylindrical shape for providing this fast hit information in the central tracker. This proposal complements conceptual designs of an EIC detector that have earlier proposed cylindrical micromegas detectors to perform this function. The potential advantage of the μ -RWELL approach is that cylindrical μ -RWELL detectors are possibly simpler and cheaper to manufacture on a large scale than cylindrical micromegas.

A microwell detector is an MPGD that is a derivative of a GEM detector. It features a single kapton foil with GEM-like conical holes that are closed off at the bottom by gluing the kapton foil to a readout structure to form a microscopic “well” structure (Figure 37, left). As with all single-stage amplification structures, discharges are a potential concern here. A resistive microwell detector addresses the discharge issue by placing a resistive layer, typically a diamond-like carbon (DLC) layer, between the well and the readout strips or pads (Figure 37, left). This structure is less complex than a Triple-GEM that requires multiple stretched foils or a micromegas that requires a micromesh and it can be produced as a single unit with the readout structure. It also spreads out the induced charge. Flat prototypes on the 1m-scale developed on PCB readouts for CMS have shown stable gain up to 2×10^4 , full efficiency, good time resolution of ~ 6 ns, and rate capabilities up to 100 kHz/cm^2 , i.e. quite appropriate for application in an EIC detector.

The main challenge for our proposed R&D project is to make the μ -RWELL into a cylindrical structure, which has not been done before. We plan to do this by implementing the readout structure on a foil instead of on a PCB to make the entire amplification and readout structure flexible so that it can be mounted on a low-mass cylindrical support structure (Figure 37, right). If this approach works, there should be no principle limit to the size of the cylinder for which this can be done since the kapton base material can be made arbitrarily long in one dimension. This would then allow the manufacturing of a continuous large μ -RWELL ring that could surround the vertex detector and possibly even the TPC in an EIC detector.

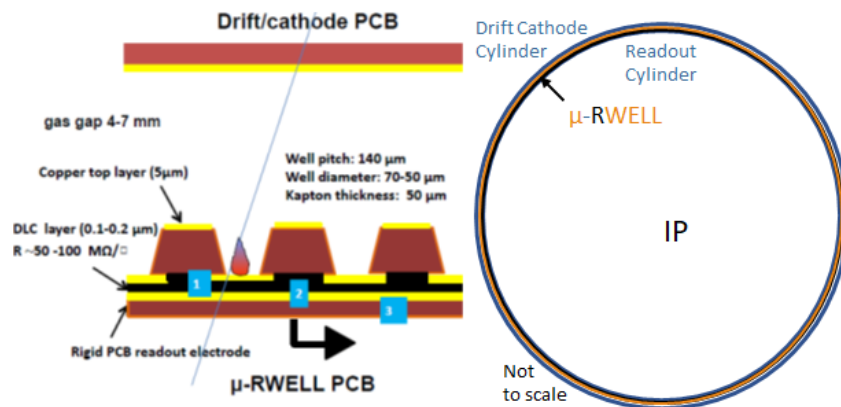


Figure 37 Left: Cross-section of a μ -RWELL detector developed by G. Bencivenni et al. (2015 JINST 10 P02008). Right: Conceptual design of a cylindrical μ -RWELL detector.

In the development of the flexible μ -RWELL we will draw on the experience we are currently gaining with the large flexible readout foil for the forward tracker at Florida Tech and UVa. Another application of experience gained from our EIC forward tracker R&D project to the cylindrical μ -RWELL would be the design of an economical readout structure for the μ -RWELL with zigzag strips or a new 2D readout design using chevron/zigzag patterns (Figure 38) being proposed by UVa in synergy with their development of high performance 2D readouts for the radial TPC detector for a future 12 GeV JLab experiment.

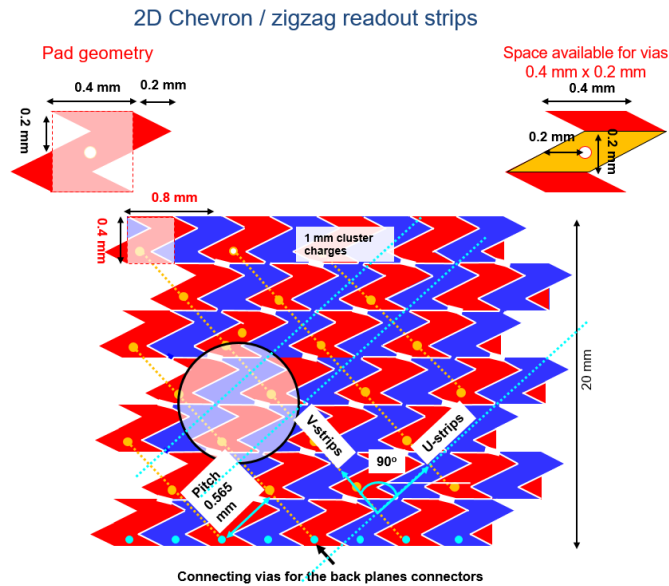


Figure 38 New idea of high resolution two-dimensional readout with chevron / zigzag strips for a cylindrical μ -RWELL detector.

Our technical approach will be to first develop small (10 cm \times 10 cm) μ -RWELL foils with zigzag or similar readouts in collaboration with the CERN workshop (Rui De Oliveira) and operate them at Florida Tech and UVa in standard 10 cm \times 10 cm Triple-GEM enclosures. We would characterize their performance including operation in mini-drift mode as studied with GEMs by the BNL group. This would constitute the entire program planned for FY2018. If it is successful, we would then design a small cylindrical prototype in FY2019.

We request \$6k for producing four 10 cm \times 10 cm μ -RWELL foils at CERN in FY2018

References:

[1] G. Bencivenni et al., “The micro-Resistive WELL detector: a compact spark-protected single amplification-stage MPGD,” JINST 10 (2015) P02008.

Stony Brook University

ION BACKFLOW STUDIES

The EIC machine is correctly characterized as a high luminosity machine for small cross section physics. Events at EIC are rather low multiplicity as compared to RHIC-heavy ion or LHC. We must address quantitatively whether and at what level ion back flow at the EIC would be an issue under the scenario of reusing all or part of the sPHENIX TPC for the EIC.

The sPHENIX TPC has been designed with goals that are antithetical to those required for the EIC. That device, pictured in the figure below, has been designed for high position resolution and low ion backflow at the cost of dE/dx resolution.

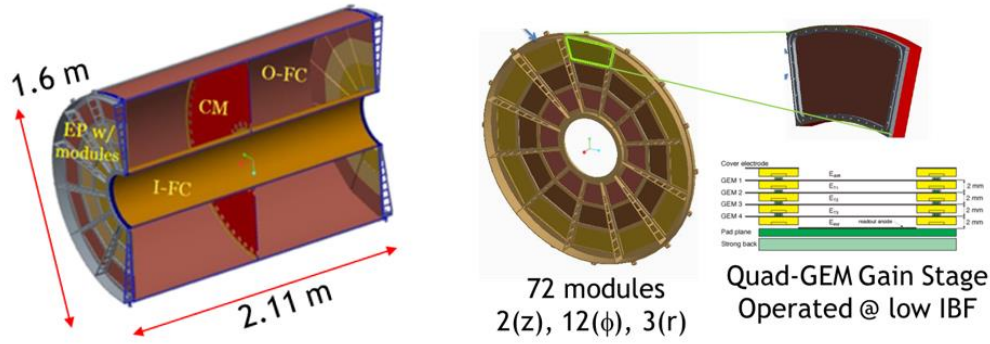


Figure 39 The sPHENIX TPC design.

The physical size of the sPHENIX field cage is, not by accident, identical to the specifications of the BeAST EIC detector design. This was intentional as a means of achieving eventual use of the device at EIC either in an evolved ePHENIX experiment, or as the volume tracker for BeAST. That said, both the differences in the RHIC heavy ion tracking environment, and the wholly different physics goals of sPHENIX from EIC have driven the particulars of the design to be not optimal for EIC. Put simply, sPHENIX cares only about momentum resolution for particles in the central region. Conversely, EIC cares principally about dE/dx resolution and pattern recognition, and further requires strict material budgets in the end caps as well as the barrel.

It is instructive to follow the decision tree to the four principle design drivers for sPHENIX to understand how these must be changed for EIC. The present sPHENIX design assumes a Au+Au collision rate of 100 kHz along with the known machine backgrounds at RHIC. Ordinarily a TPC device would be rendered useless in this environment due to electric field distortions created by positive ions loading the gas volume. Analytically, one can model the space charge density in the TPC volume as:

$$\rho(r, z) \propto \frac{\text{Ionization} * \text{Multiplicity} * \text{Rate}}{v_{ion}} \left[\frac{1 - \frac{z}{\text{Length}} + C}{r^2} \right]$$

Here the $\left(1 - \frac{z}{\text{Length}}\right)$ term comes from ionization created by the primary particles which peaks at the central membrane, and the C term comes from Ion Back flow. For a traditional TPC, the Ion Back Flow was addressed via a “gating grid” that blocked positive ions from the avalanche stage from entering the drift space. This imposes a both severe rate limitation to the device and a requirement that the detector provide a fast trigger to operate the gate. Neither of these are suitable for EIC. In addition to high rates of collisions at the maximum EIC luminosity, we note that modern electronics systems are all evolving towards a triggerless readout structure wherein local thresholds are applied to every channel and that time-tagged data for over-threshold hits are reported continuously. In such a system, a commodity computer farm is then used to assemble events. We must assume that by the time of EIC, any detector system we propose must be at least compatible with this readout scheme. The design of the ALICE TPC upgrade addresses these goals as will be shown below. For the purpose of this discussion, we shall follow the analytical space charge density formula term-by-term to set the framework for the sPHENIX operating points and specifically what must be changed and how to make the device viable for EIC.

Given some experimental condition provided by the accelerator (multiplicity, rate), the design of the TPC can only address three issues to minimize space charge:

1. Primary ionization density (*Ionization*).
2. Positive Ion Drift Velocity (v_{ion}).
3. Ion Back Flow Fraction (C).

Addressing primary ionization and positive ion drift velocity are fortunately for sPHENIX (unfortunately for EIC) a positive correlation. Using the lowest Z noble gas component in the mixture will not only lower the ionization density, but it will improve the positive ion drift velocity. Positive ion drift follows the formula:

$$v_{ion} = KE$$

where K is the mobility and E is the electric field. For all reasonable values of drift field, the positive ion mobility is constant and therefore we can maximize the velocity by using a strong drift field. Also, we maximize drive velocity using the lowest mass gas as indicated by the figure below:

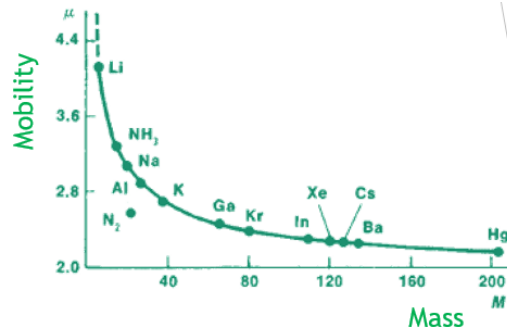


Figure 40 Positive ion mobility as a function of mass of the ion.

Finally, we can minimize space charge distortions using the fact that these maximize at the field cage boundaries as shown in the figure below:

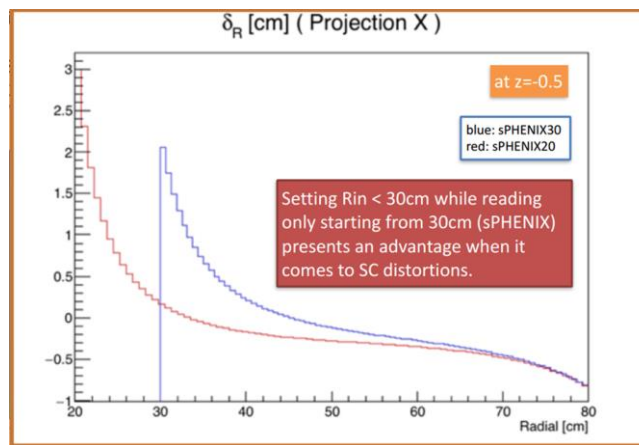


Figure 41 Space charge distortions vs radius for two different field cage configurations. The red line indicates a field cage from 20-80cm and the blue line indicates a field cage from 30-80 cm.

sPHENIX uses a field cage that begins at 20 cm, but only registers hit points from 30 cm. Thereby the distortion falls to 3mm instead of 2 cm at the innermost measured point.

As indicated in the figure, it is envisioned to replace the traditional gated wire stage with Micro Pattern Gas Detectors (quad GEMstack) running a gateless mode wherein the Ion Back Flow is intrinsically small. The ALICE goal is 1% IBF which, running at a gain of 2000, means that the space charge from IBF outnumbers the space charge from primaries by a factor of 20:1. Shown in the Figure below is the published result from ALICE on their Ion Back Flow studies:

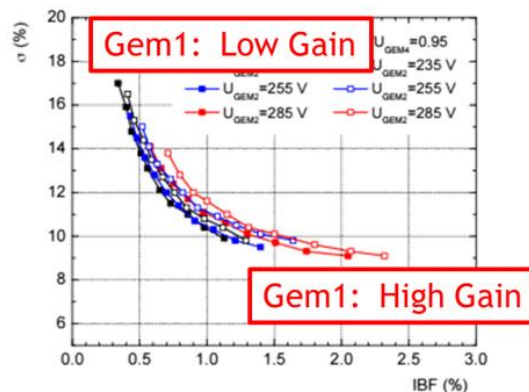


Figure 42 Energy Resolution vs. Ion Back FLOW for the ALICE gain configuration.

The vertical axis tracks the dE/dx resolution (measured as the sigma of the ^{55}Fe peak as a percentage of its width) vs. the Ion Back Flow. The tradeoff is obvious and easy to understand. Ions from the first GEM avalanche are coupled directly into the TPC volume and thereby set an absolute minimum to the IBF. Lowering the gain in the first GEM thereby lowers IBF. However, the fluctuations at low gain destroy energy resolution. sPHENIX has selected an operating point at the far left edge of this curve, which destroys energy resolution. This is antithetical to the EIC goals, wherein energy resolution and pattern recognition are the primary goals of the large volume tracker.

In summary, the sPHENIX approach to space charge relies upon the following list of design choices:

1. Minimize the primary ionization using low-Z gas.
2. Maximize the ion velocity using low-A gas.
3. Use only the track space points far from the field cage.
4. Minimize the IBF using an operating point that sacrifices energy resolution.
- 5.

None of these options is viable for EIC. To get the highest dE/dx resolution, we will need to maximize the ionization density which will certainly slow the ion velocity. We must operate the GEMstack at a range the yields superior energy resolution. EIC requires that tracking extend to the forward direction and therefore we cannot tolerate a purposeful dead area.

To compare the challenge of EIC space charge distortions to that of sPHENIX, we must scale the problem according to all the factors in the space charge density formula (repeated here for convenience) that differ between the two experimental conditions:

$$\rho(r, z) \propto \frac{\text{Ionization} * \text{Multiplicity} * \text{Rate}}{v_{ion}} \left[\frac{1 - \frac{z}{\text{Length}} + C}{r^2} \right]$$

The “figure of merit” by which we evaluate the challenge faced by any next-generation TPC is thus formulated by evaluating:

$$FOM = \frac{\text{Ionization} * \text{Multiplicity} * \text{Rate}}{K} \text{DeadVolumeFactor} * \text{OpPointFactor}$$

During the Philadelphia meeting, calculations of rates at EIC as well as first estimates of backgrounds were presented. These are the results of eRD19 and are summarized in these tables:

Machine Design	p+H ² cross section [mb]	Background Lumi [x 10 ²⁹ cm ⁻² s ⁻¹]	e+p cross section [mb]	Machine Lumi [x 10 ³³ cm ⁻² s ⁻¹]
Linac-ring (low risk)	60	1.8	0.05	1.2
Linac-ring (ultimate)	60	1.8	0.05	14.4
Ring-ring (baseline)	60	2.0	0.05	1.1
Ring-ring (ultimate)	60	4.1	0.05	12.4

Machine Design	Background rate [kHz]	DIS rate [kHz]	Physics/BG ratio
Linac-ring (low risk)	11	58	5.3
Linac-ring (ultimate)	11	700	64
Ring-ring (baseline)	12	53	4.4
Ring-ring (ultimate)	25	603	24

Figure 43 eRD19 estimates for collision rates and Beam-Gas backgrounds.

From these calculations, we can extract the DIS+Background rates for the baseline and ultimate machine luminosity as 69 kHz and 711 kHz respectively. We recognize that the background from these estimates is limited to only beam-gas interactions and misses the significant terms for Brehm and back scattering. The multiplicity per event is drawn from the calculation in the figure below with a result of 0.45 particles per unit rapidity averaged over the barrel region.

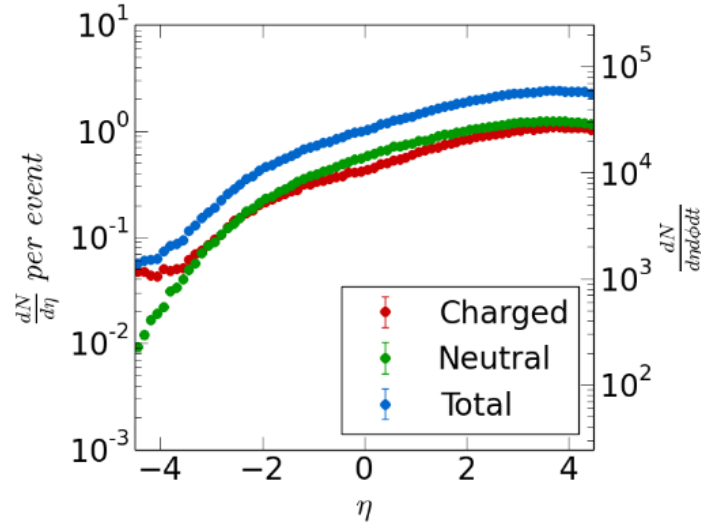


Figure 44 Multiplicity of produced particles per event at EIC. Averaged over the central barrel acceptance yields 0.45 charged particles per event.

To complete the comparison of sPHENIX conditions to EIC, we shall assume Neon and Argon gas (respectively) to calculate ionization density and ion velocity, we shall take the measured dead space factor from 0.1 (sPHENIX) to 1.0 (EIC) to track over the full detector volume, and we shall restore the operating point of the GEMstack to 2% IBF which is the plateau in energy resolution for the ALICE result. We can then evaluate the figure of merit for both sPHENIX and EIC to produce the results from the table below.

	AuAu 200 Gev	EIC (baseline)	EIC (Ultimate)
Gas	Neon	Argon	Argon
Ionization (e/cm)	43	94	94
Multiplicity	450	0.45	0.45
Rate	100	69	711
K	6.93	1.96	1.96
Dead Volume Factor	0.1	1	1
Op Point Factor	0.3	2	2
FOM	8377	2978	30689
FOM relative to sPHENIX	1.00	0.36	3.66

Figure 45 Ion Back Flow Figure of Merit for sPHENIX as compared to EIC. Large figure of merit indicates a more challenging environment.

Despite the prior assumptions made by the authors of this report (if sPHENIX solves IBF, then EIC is good to go), the process of re-optimizing a TPC for the principle task of dE/dx measurement results in 0.36X the challenge for baseline EIC and 3.66X for the ultimate EIC. Weighing these factors against the realization that synchrotron radiation backgrounds are not yet included in the EIC estimates proves that the ultimate EIC TPC device must do more than sPHENIX to achieve the same level of position distortion. Fortunately, we have additional ideas for EIC R&D that will address this issue.

Given that the gas change for EIC is critical to meeting the physics goals, the only open source of R&D to improve the IBF situation lies in breaking the “universal” IBF curve from ALICE. To understand how to break past this curve we must first understand its origin.

As stated earlier, low gain multiplication results in large fluctuations. Indeed, taking simple Poissonian statistics wherein the variable equals the mean, the fractional error falls with 1/mean. However, for a VERY LOW gain avalanche process,

we must be more careful. While the Poisson correctly rules the number of clusters the full yield of electrons from the avalanche must also include the original electron itself. This is illustrated in the trivial calculation below:

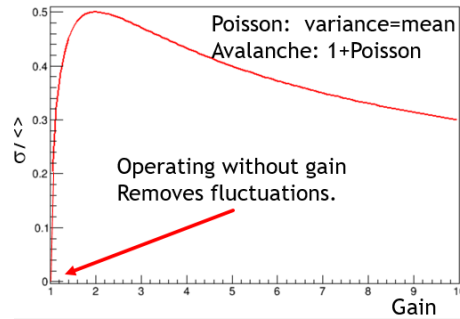


Figure 46 Fluctuation calculation including the primary electron with an assumption of transmission=1.

Simply put, an ideal transmission grid with no gain introduces no fluctuations. However, such a simple device CAN combat IBF, thereby breaking the ALICE “universal curve”. It is instructive to understand how IBF works for MPGD detectors in the overly-simplistic limit of no diffusion.

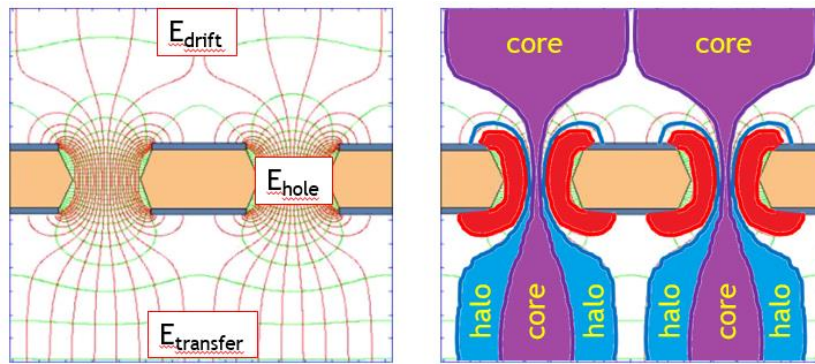


Figure 47 Simplified electron transport through a GEM.

The above classic figure shows the electric field configuration for a GEM. Here, the E_{hole}/E_{drift} ratio is sufficiently large that 100% of all electrons enter the hole. Furthermore, with $E_{transfer}/E_{drift} > 1$, we minimize the number of field lines that land on the bottom side of the GEM. Viewed from below, however, the halo region consists of field lines that terminate on the GEM rather than transmit through the hole. This is the principle mechanism behind low IBF from MPGD devices. The reason why μ MEGAS are a favored device is that their field ratio is exceptionally high.

The fundamental relationship of IBF to $E_{transfer}/E_{drift}$ can be exploited by other structures even simpler than a GEM. We have performed Garfield calculations for a simple mesh grid to calculate both the percentage collection of electrons and the percentage blocking of ions with the results shown below.

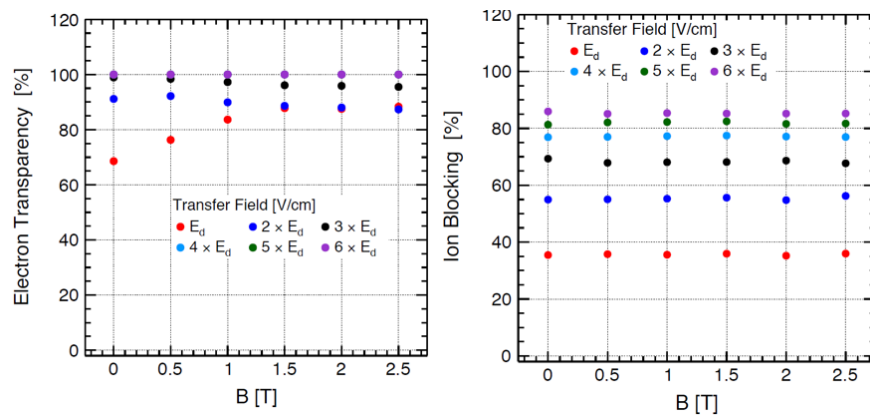


Figure 48 Electron transmission (left panel) and ion blocking (right panel). Large values of each are desirable and easily achieved with proper field ratios.

The mesh simulated here has 500 micron holes and 30 micron wires. Calculations are full transport with diffusion as well as the presence of a magnetic field. The results are quite remarkable and indicate that new structures can do much better than the ALICE curves. As part of our EIC-specific TPC R&D we wish to perform bench tests of this phenomenon at Stony Brook to pursue a better figure of merit than sPHENIX to enable the use of the TPC at the ultimate EIC luminosity. We will use both equipment borrowed from Yale as well as newly purchased devices for these measurements.

Joint R&D Proposal Stony Brook University/Bonn University/DESY

We propose to develop a novel readout system which is based on broadly available readout chips for Silicon pixel detectors. These chips (for instance the Timepix chip) offer the functionality of a TDC readout per channel in a highly integrated package. Our experience is coupled to the Timepix ASIC, which features 256 x 256 pixels with a pixel pitch of 55 μm x 55 μm . Each pixel can record either the time of arrival or the charge collected (time over threshold mode). We propose to combine the Timepix chip with a traditional pad plane, to allow for larger pads and thus coverage of a larger area.

Introduction

In the scope of the EIC physics program, semi-inclusive deep inelastic scattering (SIDIS) reactions in e-p, respectively e-A collisions play an important role regarding the spin of the proton, Fragmentation Functions (FF), Transverse Momentum Distributions (TMDs) by means of flavor tagging through hadron type, measuring Kaon asymmetries and cross sections, measuring strangeness Probability Distribution Functions (PDFs), amongst others. This, in turn requires p^\pm , K^\pm , p^\pm separation over a wide range in pseudorapidity, $|\eta| < 3$. It needs to cover the entire kinematic region in p_t and z , needs excellent particle identification (PID) and excellent momentum resolution at forward rapidities. TMDs need full azimuthal coverage around the virtual photon and a wide p_t coverage. For identifying hadrons, the technique via energy

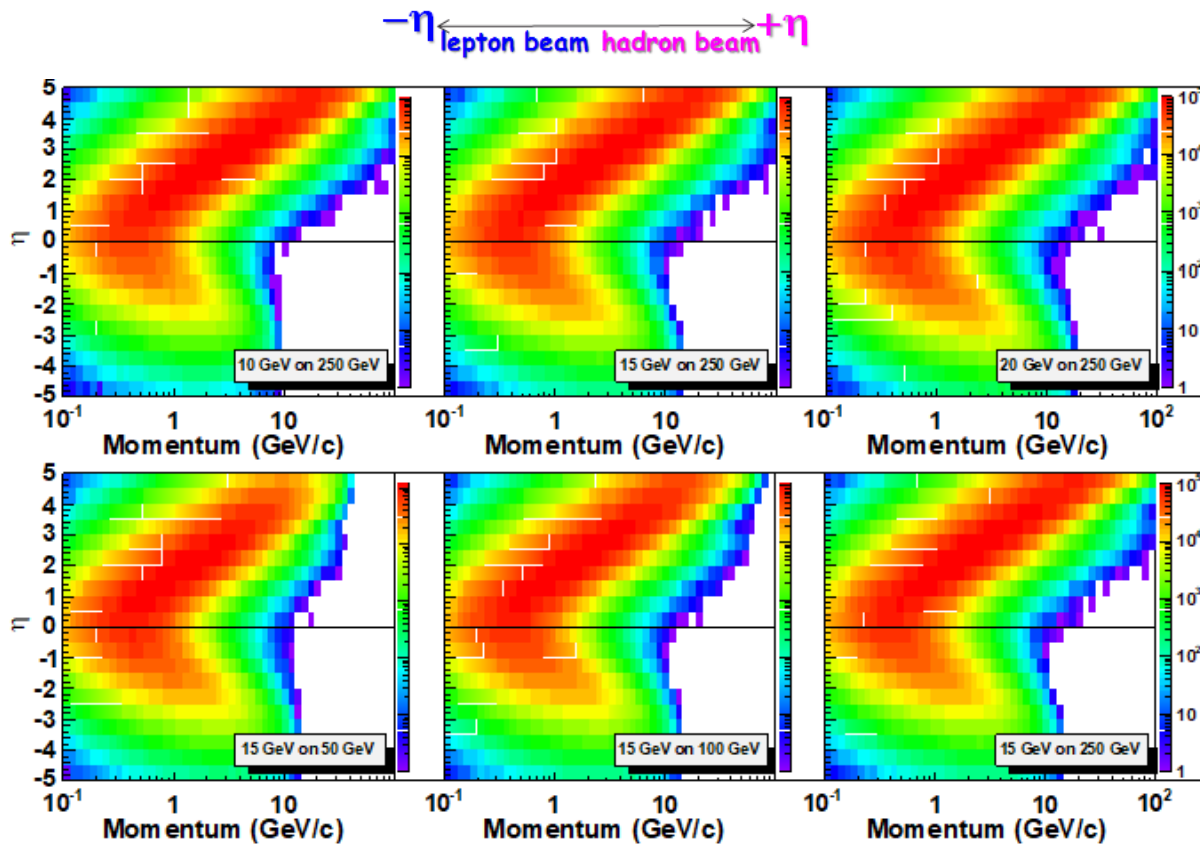


Figure 49 Pion kinematics in SIDIS. Upper: collisions with increasing lepton-beam energy and fixed hadron-beam energy, where hadrons are increasingly boosted toward negative pseudorapidities. Lower: collisions with increasing hadron-beam energy and fixed lepton-beam energy, where hadrons' momentum at fixed pseudorapidities increases. It shall be noted that other hadron species beside π^\pm , like K^\pm and p^\pm show the same kinematics.

loss in the detection medium - dE/dx - with the combination of Ring Imaging Cherenkov (RICH) Counters can be used. They must cope with a π/K ratio of 3 - 4, and a K/p ratio of 1.

Figure 49 shows that in mid-rapidities a significant fraction of produced pions (K, p) have momenta from lowest to about 1 - 3 GeV/c. The principal idea of a Time Projection Chamber (TPC) is the combination of tracking and PID in a single detector. Gas ionization by a charged particle depends only on its velocity and the square of the charge but not on its mass. PID can, therefore, be achieved by simultaneously determining the particle momentum and its velocity from the ionization. When speaking of dE/dx ; more precisely the localized ionization deposited near the track. This allows, in general, to distinguish between electrons/pions and amongst hadrons, at low momenta up to about 3-4 GeV/c, very well suited to perform PID tasks in mid-rapidities.

PID WITH A TPC

For particle separation, precise knowledge of two parts is required: the general dependence of dE/dx on the velocity and the ionization deposit along a specific track. The ionization loss drops as $1/\beta^2$ for low $\beta\gamma$ goes through a minimum for $\beta\gamma = 3-4$, then rises logarithmically in $\beta\gamma$ (relativistic-rise region) until it reaches a plateau. PID is easy in the $1/\beta^2$ part but difficult in the relativistic-rise region. The dE/dx curve and in particular, the slope of the relativistic-rise region and the plateau depend mainly on the gas and its pressure but also on the method used to measure the ionization. This function has to be determined from fitting the dE/dx measurements for well-identified particles in different $\beta\gamma$ regions, such as Bhabha electrons, cosmic muons and minimum ionizing pions. The measurement of the energy loss of charged particles traversing the volume of a TPC is traditionally performed by counting the charge from the ionization deposited along the track. To measure the ionization loss of a particular track with reasonable precision, many samples have to be taken on the track. Ionization resolution is continuously improving with increasing number of samples for a given track length. So-called

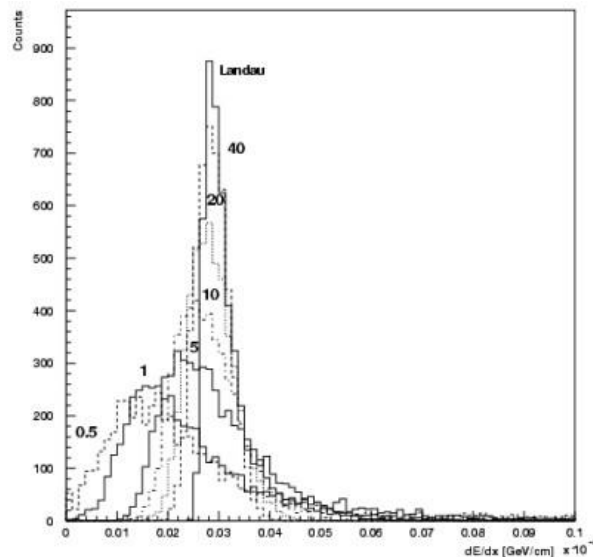


Figure 50 Energy loss distribution for a 3 GeV electron in Argon simulated with GEANT. The width of the layers is given in centimeters. The energy loss can readily be converted into a number of electrons [1].

straggling functions (Figure 50) are providing typical energy loss distributions. They have long tails which are caused by so-called δ -electrons.

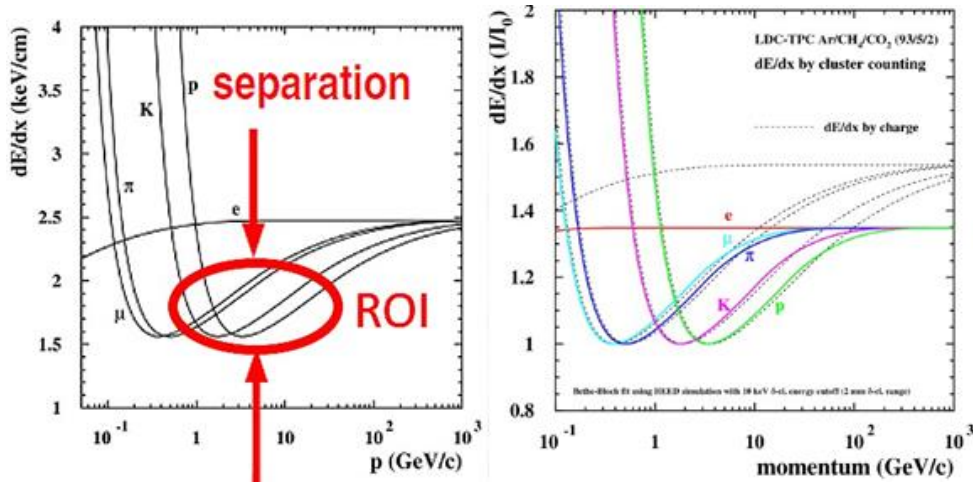


Figure 51 Left: Energy loss from the modified Bethe-Bloch function [2]. The region of interest (ROI) can be enhanced if the proper separation in the ROI can be provided. Right: Comparison of energy loss from the modified Bethe-Bloch function, for charge measurement (dashed lines) and with cluster counting (solid lines).

Those have received a rather large amount of energy by the ionizing particle and allows them to further ionize atoms/molecules in the gas making them appear to be an ionizing particle by itself. These electrons lead to large fluctuations of the measured charge and further let the mean and the variance of the distribution become ill-defined. A more reasonable description is given by the most probable ionization I_{mp} and the FWHM. The procedure most widely used is the calculation of a truncated mean, denoted as I , as the mean of the lowest $p\%$ (typically $p = 60 - 80$) of the pulse heights. The cut reduces the effect of fluctuations due to the long tail. However, the cut also removes a fraction of track samples which in turn worsens the ionization resolution. Instead, it is of advantage to count the number of clusters the incident particle releases along its track. This is given by a Poissonian distribution with a significantly smaller width, resulting in a better correlation and particle identification power. To be more accurate, one has to consider particle separation power instead of ionization resolution. The separation of two particle species in dN/dx in units of the dN/dx resolution can be described by separation power = separation/resolution. Figure 51 - Figure 54 and the following examples are based on calculations for the LDC-TPC [3] read out with triple-GEM detectors, with Ar-CH₄-CO₂ (93-5-2) counting gas and 120 cm track lengths. Figure 51 shows that the momentum range for PID with a TPC can be quite enhanced if the separation can be achieved accordingly.

The Bethe-Bloch function differs when one is considering the two different techniques of obtaining dE/dx via charge counting and cluster counting (Figure 51, right). The difference stems from the fact that the charge measurement is highly sensitive to secondary electrons, which are increasingly abundant at higher momenta due to δ -electrons. They are ignored if cluster counting is (perfectly) performed. The relativistic rise is truncated because the Fermi plateau is reached much earlier with cluster counting, but particle separation stops therefore at lower momenta. The shape as well as magnitude of particle separation power, however, differ significantly (Figure 52). Cluster counting allows for a maximum separation at slightly larger momenta as compared to charge counting. It provides more separation below and less separation above certain momentum as compared to charge counting. The π/K separation power as shown in Figure 53 indicates that a 50% efficiency performs significantly better than the separation power obtained with charge counting. Even a 20% efficiency can compete with charge counting. In previous experiments with prototypes, a cluster counting efficiency of only 20-30% has been reached. However, as shown above, the resulting separation power is still better than by charge summation. Also, improved algorithms are expected to deliver a higher cluster counting efficiency. On the other hand, cluster counting can only work if a sufficient correlation between the position of the electrons of one cluster is preserved during drift. A perfect cluster counting efficiency of 100% is virtually impossible since the transverse diffusion of the electrons for effectively all gas mixtures will result in merging of clusters along the drift length of the electrons. Details needs to be investigated with simulations.

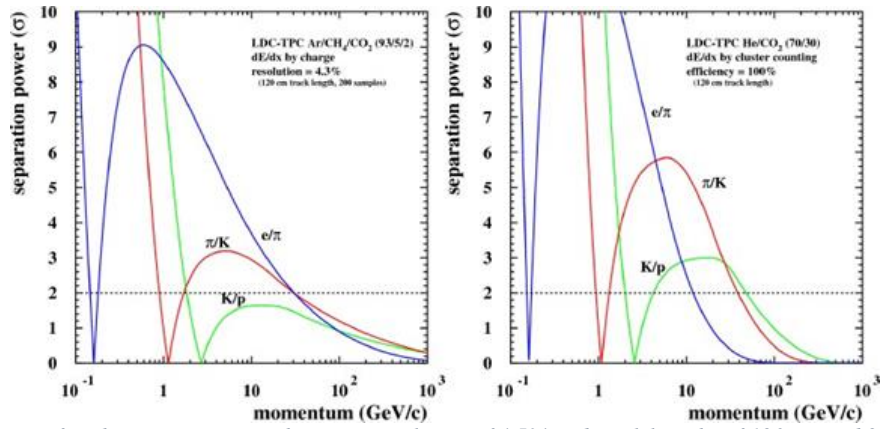


Figure 52 Left: Separation power for charge counting, with energy resolution of 4.5% and track lengths of 120 cm and 200 samples along the track. Right: Separation power for cluster counting, for the same gas and track length as Left. A 100% counting efficiency is assumed.

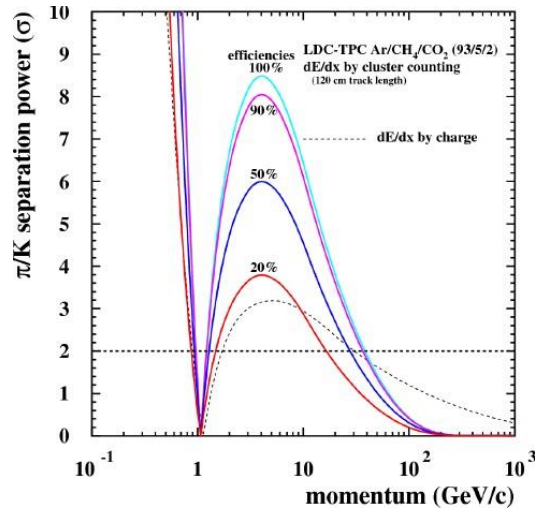


Figure 53 Separation power for π/K with cluster counting, based on different counting efficiencies (solid lines), compared to the separation power with charge counting.

DESCRIPTION OF A NOVEL READOUT DESIGN

Modern gaseous detectors increasingly utilize micro-pattern gaseous detectors (MPGD). These systems, of which there are several derivatives, are characterized by amplification structures that are of a size similar to the intrinsic spatial resolution of $O(100 \mu\text{m})$ or smaller. These systems are read out either with pads, typically of a width of 1 mm or similar, or, as the extreme other case, with pixels of a size of $50 \mu\text{m}$ by $50 \mu\text{m}$. In the traditional case a pad plane is prepared, through which the signals are routed to a readout system. To fully exploit the information of the pads the readout system quickly renders complex, and typically contains charge sensitive pre-amplifier and a fast analog to digital converter (FADC) to measure time and charge of the pulses. The pixel based readout on the other hand collects only minimal information per hit, usually time, based on a simple time to digital converter (TDC) circuit, whether a hit has occurred or not, and possibly charge. In the traditional case the challenge is to develop the electronics with a small enough footprint. In the pixel case, the challenge is to handle the large number of channels needed to instrument significant areas. Studies done over the past years have shown that a TDC based simplified readout can reach very similar resolutions as have been obtained with the FADC based approach.

To achieve the cluster counting capability, a sufficiently high granularity is needed for the TPC readout system. A comparison of two existing prototype systems is shown in Figure 55. The electron clusters are amplified by Gas Electron Multipliers (GEMs), creating charge clouds visible as blue blobs. The anode consists of 8 Timepix ASICs with their pixels as immediate sensitive anode, which has a pitch of $55 \times 55 \mu\text{m}^2$. The charge clouds are clearly identifiable – the granularity is even higher than needed, causing more data than necessarily required. On the other hand, the green overlay of a typical current pad-based readout system shows, that with its pads of about $1 \times 6 \text{mm}^2$ cluster identification is not possible.

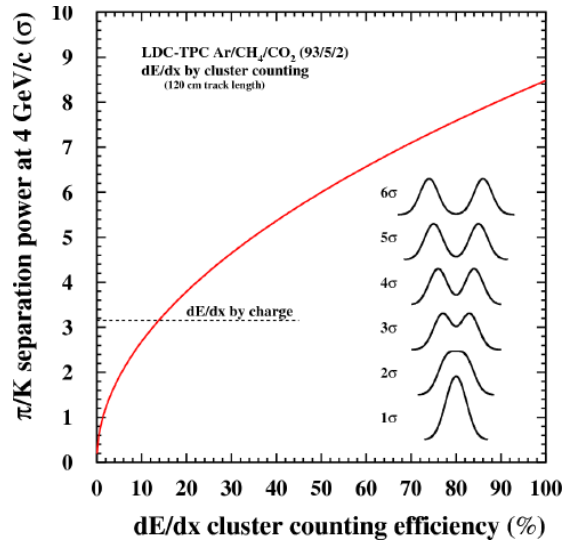


Figure 54 Separation power for π/K at $p = 4$ GeV/c, with cluster counting, improving with increasing counting efficiency. The right insert depicts a graphical representation of the various separation powers. The dashed line indicates the separation power with traditional charge counting.

In addition to the cluster counting capability of such approach one has a significantly reduced amount of material in forward direction as the readout electronics is concentrated on a rather small area. For the Timepix chip 65,536 channels on an active area of about 2 cm^2 . This is a very promising aspect for an EIC detector since one can significantly reduce material in the direction of forward scattered particles, across a TPC end plate, in particular in the direction of the scattered electron.

PROPOSED STUDIES

We propose to develop a novel readout system which is based on the Timepix chip that offers the functionality of a TDC readout per channel in a highly integrated package. This proposal is based on an earlier work reported in [5]. The aim is to confirm expected results and to develop an advanced end plate (ceramic or silicon) based on the findings.

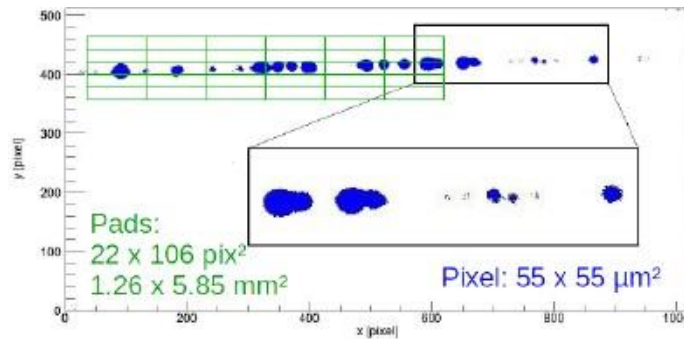


Figure 55 Event display of a track recorded with a Timepix Octoboard [4]. The activated pixels are shown in blue, the green overlay shows the pitch of a typical pad-based readout.

Each pixel of the Timepix ASIC can record either the time of arrival or the charge collected (time over threshold mode). We propose to combine the Timepix chip with a traditional pad plane, to allow for larger pads and thus coverage of a larger area. Pad sizes will be around $300 \mu\text{m}$ to enable cluster counting, to give a large flexibility and to keep the channel number low at the same time.

As depicted in Figure 56 GEMs will be used for amplification, small pads on a PCB form the anode and are read out by a Timepix ASIC. The connections from the pads are routed through the PCB to the ASIC which is bump bonded to the PCB surface, that needs to be sufficiently flat.

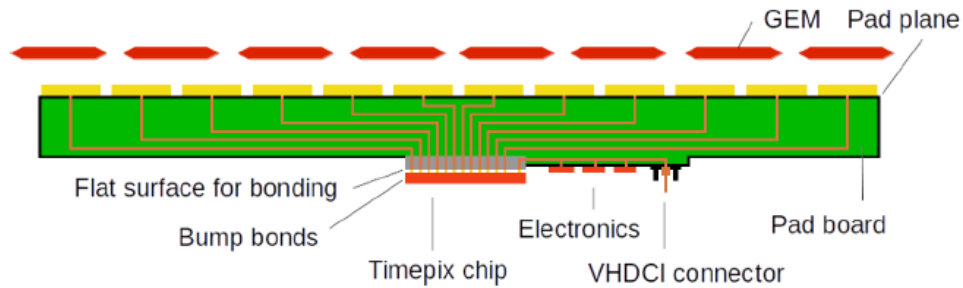


Figure 56 Structure of the proposed readout system.

Concerning technology, it is pioneering work to connect a pixel chip with such a small pitch directly to a PCB. The Timepix power and communication pads are on the same side of the ASIC as the pixels. They are usually connected by wire bonds. In the proposed approach these pads have to be connected by bump bonds to the PCB, which also hosts the further electronics elements including the connectors for the chip voltage supply and an I/O-cable plug. The data processing is conducted by a Scalable Readout System (SRS) developed by the RD51 collaboration at CERN. A Front-End Concentrator card (FEC) hosts a Field Programmable Gate Array (FPGA) that reads the data from the Timepix ASIC via an adapter card and a VHDCI-cable to the readout board. The FEC can be connected via Ethernet to a PC. Compared to traditional pad-based systems our approach will have a higher granularity leading to charge cloud and possibly cluster identification capability beside improved double hit/track resolution and reduced occupancy. In addition, the Timepix ASIC allows for a significantly smaller footprint of the readout electronics.

Traditional pixel-based systems, e.g., the InGrid system [6], have a higher granularity and record each electron with exactly one pixel. Pixel granularity combined with a GEM [7], does not increase the performance, but only the data output. Because the ASICs need some overhead area, and the module geometry, foreseen for cylindrical TPCs is not square like the ASICs, a pixel-based anode can currently cover only about 50% of the anode area in a setup with 12 Octoboards [8], or up to 63% with tightly stacked ASICs as suggested in [9].

Our approach measures each primary electron with several pads, allowing for position calculation using a fit. Furthermore, our approach allows to separate anode PCB and consequently for a coverage of more than 90% area, comparable to the traditional pad-based systems. Also, it is more flexible with regard to the granularity, since for a desired change in pad size it is required to only produce new PCBs and bond them to the ASICs, not to produce new ASICs with a different pitch.

The input capacitance of the pixels is a challenge for this project. Usually, pixel chips are bonded to sensors with the same pitch and small conductor volume and thus a small capacitance per sensor channel. Therefore, the Timepix ASIC is made for input capacitances below 100 fF, see Figure 57 [10]. In our approach, each connection goes through the board, and the capacitance is dominated by the line length with a value around 1 pF / inch. The pads and the bump bonds add only around 100 fF to the input capacitance. For line lengths between pad and pixel in the order of cm this clearly reduces the expected signal to noise ratio to a difficult level. This can probably be mitigated by an increased gas amplification in the GEM stack, leading to a signal of up to several 10k electrons. Overall, a solution to the capacitance challenge seems feasible and will be investigated with a testboard.

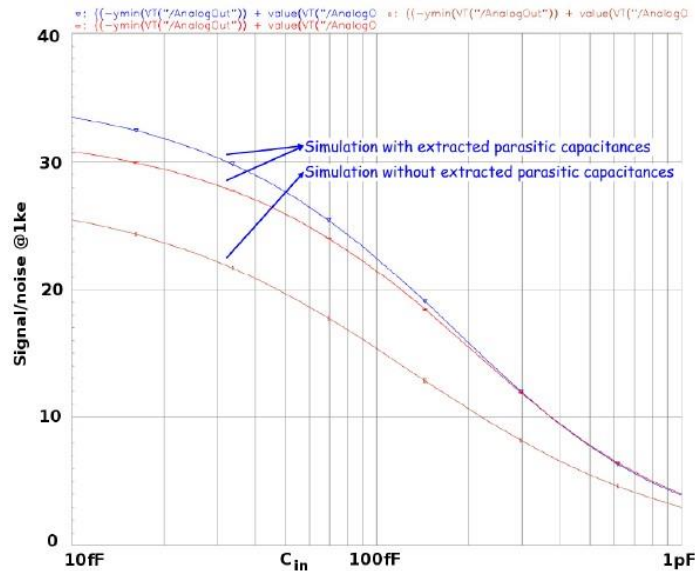


Figure 57 Simulated signal to noise ratio of the Timepix chip as a function of the attached input capacitance.

Summary of challenges

- the Timepix chip is optimized for a low input capacitance (10-100 fF). Once connected to a pad plane a much higher capacitance will be present at the input (1-20 pF). We will need to establish whether the system will function in this configuration.
- the Timepix chip with its small pixels will need to be connected to the readout plane. This requires sophisticated and highly non-trivial interconnection technology. This must be done by bump bonding, which is regularly performed when connecting readout chips to silicon sensors. However, when connecting to a PCB, the usual and established technology is available only for significantly larger pitches.
- the routing on the PCB between the bump bond pads and the charge collection pads is non-trivial, and will need great care and advanced production techniques.

Summary of advantages

- + the footprint of the readout will be much reduced
- + the power consumption will be much reduced
- + significant decreased material budget in forward direction
- + the system will be significantly cheaper than a traditional one
- + the system offers the possibility to reduce the size of the pads significantly, to profit from the increased precision, without having to go to the extreme case of pads of the size of the pixels on the chip.

R&D PROGRAM

The R&D program is anticipated to be performed within two years.

A first test setup with a Timepix chip does exist at DESY which is based on a system that has been prepared in Bonn. A simple PCB has been produced and successfully bonded to the Timepix chip at the Karlsruhe Institute of Technology (KIT). As soon as this board will arrive at DESY it will be equipped for performing first tests. It is anticipated that first conclusions can be drawn regarding feasibility and performance shortly after. A simulation of the system is currently being developed at DESY that will answer questions concerning cluster counting and related problems.

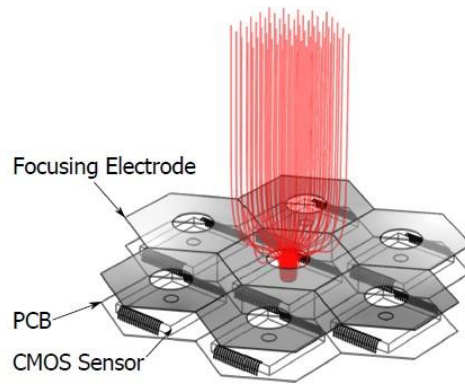


Figure 58 Focusing the charge signal onto "fractional" pads, thus decreasing capacitance but maintaining the overall pad size.

In the first year a simulation study will be performed to establish the optimal size of the pads, for best resolution, with the largest possible pad size, adapted to the compact size of an EIC-TPC. In a small setup, routing technologies will be developed for very low charge signal by comparing simulation results with some dedicated electrical tests, based on various approaches. From these studies, also conventional readout pad planes could profit. Using standard PCB technology small prototype readout planes will be built and tested to establish the best procedure. For instance, the approach of focusing electrodes will be investigated, see Figure 58. A test-of-principle experiment will be done where a few channels of the Timepix chip will be connected to the test pad-plane. This test will establish whether an acceptable signal to noise ratio can be reached, and whether the large mismatch in input capacitance mentioned above can be handled. The details of this setup will need to be developed, and in particular ways to connect the pixels on the chip will be tested. In this step also first connection techniques, like gold stud bumping or solder bump bonding will be tested. Bump bonding experience exists at one of the collaborating institutes, University of Bonn. Bonn has extensive experience in using the Timepix chip, and has pioneered the use of this chip in a TPC. DESY and SBU have extensive experience in developing traditional pad-based TPC/HBD/RICH with GEM readout systems.

In the second year, the main development will aim to work with a still limited but larger number of pixels of the chip. The pixels will be bonded to a prototype pad plane. Potentially a plane with a number of pads of $O(\text{few } 1000)$ could be considered, which would be enough to cover a significant area in an existing prototype TPC, and would allow a first realistic study of reachable precision in this readout configuration. For this step, different technologies for the pad plane could also be investigated. A very promising option might be the use of low temperature co-fired ceramics (LTCC) for the readout. This would allow for a very flat pad plane (which is required to allow reliable bump bonding of the chip to the plane), excellent thermal properties to handle the heat of the chip and companies exist that offer an integrated pipe for cooling fluids such as two-phase CO_2 . Also, the micro-via technology could be important to reach the high pad density on the PCB.

The main goal is the development of a pad-plane which can make use of the granularity of the readout system. The material of the pad-plane is also a subject of investigation, e.g., the option to use ceramic, as mentioned above or silicon material for pad planes is under consideration and might also offer the possibility to integrate miniaturized cooling systems. Other pixel readout electronics than the Timepix chip will be investigated which might result in a less sophisticated readout plane. Chips like the FEI4 [11] or considering the adaption of the Topmetal [12] chip will be investigated.

References

- [1] K. Lassila-Perini and L. Urbán, "Energy loss in thin layers in GEANT", Nuclear Instruments and Methods in Physics Research A 362 (1995)416-422
- [2] C. Amsler et al., (PDG), 2008 Review of Particle Physics Phys. Lett. B 667 1
- [3] M. Hauschild, "dE/dx and Particle ID Performance with Cluster Counting", talk presented at the [ILC Ws. Valencia](#)
- [4] M. Lupberger, "The Pixel-TPC: first results from an 8-InGrid module". JINST 9.01 (2014), p. C01033.
- [5] U. Einhaus, J. Kaminski, "ROPPERI - A TPC readout with GEMs, pads and Timepix", Presented at the International Workshop on Future Linear Colliders (LCWS2016), Morioka, Japan, 5-9 December 2016, [arXiv:1703.08529](#)

- [6] M. Lupberger et al., "Toward the Pixel-TPC: Construction and Operation of a Large Area GridPix Detector", IEEE TRANSACTIONS ON NUCLEAR SCIENCE, VOL. 64, NO. 5, MAY 2017
- [7] U. Renz, "A TPC with Triple-GEM Gas Amplification and TimePix Readout".In: (2009). [arXiv:0901.4938](https://arxiv.org/abs/0901.4938)
- [8] M. Lupberger, "Preliminary results from the 160 InGrid test beam", presented at [LCTPC-WG Meeting 2015](#).
- [9] J. Timmermans, "Progress with pixelised readout of gaseous detectors", presented at [ALCPG Eugene 2011](#).
- [10] X. Llopart, TIMEPIX Manual v1.0. 2006.
- [11] M. Barbero et al., "FE-I4 ATLAS Pixel Chip Design", PoS(VERTEX 2009)027
- [12] C. Gao et al., "Topmetal-II⁻: a direct charge sensor for high energy physics and imaging applications", 2016 JINST 11 C01053

Funding requests and budget

Proposed Budget for the BNL R&D program for FY18

<i>Item</i>	<i>Cost in \$</i>	<i>-20%</i>	<i>-40%</i>
<i>Production of new zigzag readout boards</i>	<i>20K</i>	<i>10K</i>	<i>10K</i>
<i>Gas & supplies</i>	<i>8K</i>	<i>8K</i>	<i>8K</i>
<i>Materials for X-ray scanner & cosmic ray telescope</i>	<i>12K</i>	<i>12K</i>	<i>7K</i>
<i>Additional readout electronics</i>	<i>10K</i>	<i>10K</i>	<i>5K</i>
<i>Subtotal</i>	<i>50K</i>	<i>40K</i>	<i>30K</i>
<i>Total w/overhead</i>	<i>75K</i>	<i>60K</i>	<i>45K</i>

Milestones:

- *Fully funded proposed budget:*
 - Design followed by production of new zigzag PCB's, at least two iterations, including laser and possibly high precision chemical etching
 - QA measurements of fabricated PCB's for the purpose of evaluating the fabrication processes we opted for
 - X-ray scans of new zigzag PCB's, which attach a figure of merit to each design/fabricated PCB
 - Assembly of new GEM-based cosmic ray telescope, followed by in-lab absolute position resolution measurements of 4-GEM using each PCB
 - Gas studies using ALICE-style 4-GEM using various gas mixtures favorable for a TPC in an EIC environment
- *20% de-scoped project:* This budget scenario would result in our ability to only have a single iteration of zigzag PCB production, which would severely limit the depth of our studies.
- *40% de-scoped project:* This budget scenario would also result in a single iteration of PCB production with very significant limits to what may be accomplished for assembling the high-resolution GEM-based telescope.

Proposed Budget for the joint Florida Tech and UVA R&D program for FY18

	Request	-20%	-40%
μ-RWELL prototypes	6.0k\$	3.0k\$	3.0k\$
Chromium GEM foils	4.0k\$	2.0k\$	2.0k\$
Gas at FNAL and other lab materials	3.5k\$	3.0k\$	2.0k\$
Summer students: Simulations	8.0k\$	8.0k \$	5.0k \$
Travel for joint GEM test beam @ Fermilab	10.0k\$	9.0k\$	8.0k\$
Travel to Florida Tech for Cr-GEM tests	1.5k\$	1.0k\$	0.0k\$
Total	33.0k\$	26k\$	20k\$

Proposed Budget for FY18 by individual institutes

UVA

	Request	-20%	-40%
μ-RWELL prototypes	3.0k\$	1.5k\$	1.5k\$
Gas at FNAL and other lab materials	1.75k\$	1.5\$k	1.0k\$
Undergraduate student: Simul.	4.0k\$	4.0k \$	2.5k \$
Travel to FNAL & FIT	6.5k \$	5.0k \$	4.0k \$
Total	15.25k\$	12.0k\$	9.0k \$

Florida Tech

	Request	-20%	-40%
μ-RWELL prototypes	3.0k\$	1.5k\$	1.5k\$
Chromium GEM foils	4.0k\$	2.0k\$	2.0k\$
Gas at FNAL and other lab materials	1.75k\$	1.5\$k	1.0k\$
Undergraduate student: Simul.	4.0k\$	4.0k\$	2.5k\$
Travel to FNAL	5.0k \$	5.0k\$	4.0k\$
Total	17.75k\$	14.0k\$	11.0k\$

Cost reductions in -20% and -40% scenarios:

In these scenarios, the cost would be reduced with various measures. Instead of making and testing two u-RWELL foils per group, only one would be made for each group. This carries the risk that if a foil malfunctions, the group has to stop work on the project.

Instead of producing new common Cr-GEM foils, copper would be removed from existing standard common GEM foils. This option will reduce the cost by a factor of two, but carries a risk of losing a GEM foil and consequently the entire detector and the research program since CERN cannot guarantee 100% yield on the copper removal process. Only one summer student instead of two would get trained at BNL on EIC simulations of low mass forward tracking. Only three people would conduct the FNAL beam tests and Dr. K. Gnanvo, the expert on Cr-GEMs, would not travel to Florida Tech for work on the Cr-GEMs. All these measures will slow down project progress.

Funding Requests for INFN

The founding request for this R&D activity is presented in Table 3, where the bare requests are listed and also the overhead is included assuming the typical INFN rate of 20%. The request includes 3 main chapters:

- the financial support for **a postdoc (7 months)** fully dedicated to the project: the contribution of a dedicated personnel unit will offer a crucial boost to the R&D program;
- **traveling resources**, mainly to have the possibility of closer interaction with the whole eRD6 Consortium and to follow the evolution of the EIC project: 2 trips to US per year require about 6000 \$; a minor support is requested to allow travelling to and from Bari and Trieste for the common work about the ND photocathodes: this needs is estimated to be 3000 \$ per year; another minor support is requested for material procurement, to interact with the producers when non-standard components are needed and for the construction of specific detector elements that must be produced at CERN: this needs is estimated to be 3000 \$ per year;
- Consumables have to cover prototype components and prototype operation costs; the needs for the next year will be partially covered by the delayed availability of the support granted for this year. Consumables for FY2018 include:
 - Material and fabrication of THGEMs to be used as ND photocathode substrates: 2000 \$;
 - Mechanics and equipment (connectors, gas connections, mechanical frames) to test the sample photocathode in an appropriate cell comparing measurements in vacuum and in gaseous atmospheres: 2000 \$;
 - ND powder samples: 2000 \$;
 - Preparation and analysis of metallographic specimens to study the ND distribution in the holes of the THGEM substrate: 1500 \$;
 - Material transportation BARI-TRIESTE: 1500 \$;
 - Gas bottles to operate the detectors: 2000 \$;
 - Miscellanea of small items: 3000 \$.

	cost	INFN overhead	TOTAL (=cost+overhead)
	(k\$)	(k\$)	(k\$)
item			
manpower	20	4	24
travelling (3 trips to US + trips for material procurement and construction + BARI-TRIESTE travelling for the ND photocathodes)	10	2	12
consumables	14		14
total	44	6	50

Table 3 Funding request INFN

Proposed Budget Request TPC IBF Studies

Although the SBU facilities, along with equipment borrowed from our Yale colleagues, represent a quite capable R&D platform, several practical matters should be addressed. The large clean room at SBU currently hosts efforts for both the EIC Gatling Gun electron source (a joint SBU/BNL R&D project) and production/testing for the sPHENIX TPC. We will be able to perform all work described in this project if we remove the glovebox from the clean room and use the freed space to install a second clean table. As is well known, a clean table housed in a clean room is idea for any MPGD work. We have a quote from RDM industries for an 8’ clean table (same as used for prior GEM work) at \$7034. Furthermore, our excellent quality gas system will be tied up by sPHENIX activities. While we have ample spare mass flow units (in multiple ranges), we will need to buy a new controller whose current eBay price is \$1999.99. The funding request for a full-scale IBF measurement is:

	Cost	Overhead	Total	20% Reduction	40% reduction
Laminar Table	\$7,034.00	\$4,150.06	\$11,184.06	\$11,184.06	\$0.00
Flow Controller Unit	\$1,999.99	\$1,179.99	\$3,179.98	\$3,179.98	\$3,179.98
Circuit Cards	\$4,000.00	\$2,360.00	\$6,360.00	\$6,360.00	\$6,360.00
Gems/mMEGAS	\$5,000.00	\$2,950.00	\$7,950.00	\$7,950.00	\$7,950.00
pAmmeters	\$5,370.00	\$3,168.30	\$8,538.30	\$0.00	\$0.00
Consumables	\$3,000.00	\$1,770.00	\$4,770.00	\$4,770.00	\$4,770.00
TOTAL	\$26,403.99	\$15,578.35	\$41,982.34	\$33,444.04	\$22,259.98

For our cost reduction scenarios, we shall forego first the professionally made picoAmmeter in favor of a jury-rigger model designed in house. Secondly, we would give up on the laminar table and risk doing the project in the main clean room.

Proposed Budget for the joint Bonn University/DESY/SBU R&D program for FY18

All participating institutes will provide manpower with faculty, scientific staff, and graduate students. Bonn University and DESY have supporting funds which rendered possible the start of the studies as proposed here.

Faculty and staff will not request funding for labor, however, we will request funding for two graduate students; one shared between Bonn University and DESY, and one at SBU, each for the anticipated duration of the project, i.e., two years.

We are requesting funding for bonding and connection tests of the boards to be produced as well as for the acquisition of Timepix chips and others within the first year. For the second year we will be requesting funding for the acquisition of larger boards, miscellaneous hardware, travel and participating in a test-beam, but is not listed in this document.

Our baseline funding request for year 1 is summarized in the table below.

Year 1 cost item	DESY	University of Bonn	Stony Brook University	Sum
Salary graduate student	(1/2) \$25k	(1/2) \$25k	\$48.5k	\$98.5k
Board production	\$10k	\$20k	\$10k	\$40k
Timepix chip	-	-	\$5k	\$5k
Travel costs	-	-	\$5k	\$5k
Total request	\$35k	\$45k	\$68.5k	\$148.5k

Table 4 Budget request Year 1. One graduate student will be shared between DESY and Bonn University. Student requests are fully loaded.

Two reduced funding request scenarios are described.

Year 1: for a reduced budget scenario with nominal budget minus 20% the reduction would directly affect the items of board production and the acquisition of the Timepix chip. The students' salaries cannot be touched. Consequently, the board production has to be made cheaper by 50% and the acquisition of the Timepix chip has to be canceled. The cost reduction for the boards would result in the acquisition of readout boards for only one of the participating institutes and would make the project unreasonable since the production of boards are based on various technologies to be tested. In the case nominal budget minus 40% the leftover will be salaries and the project would not be possible.

Deliverables

Establish the use of a Timepix based readout for gaseous chambers.

Establish connection technology to successfully bond the Timepix to a readout plane.

Study and establish alternative technologies (e.g. ceramics based) for pad planes for possible improved mechanical and thermal properties. If successful the proposed project could substantially contribute to the development of a new generation of highly granular and affordable gaseous detector systems.

Developing routing design for optimized signal transport for very low charge signals (10^3 - 10^5 electrons) confirmed by simulations and experiments.

For a year 2 continuation of the project it is expected to produce a nominal TPC module for an EIC detector with 5000 charge collection pads connected to 1-3 Timepix ASIC and verified in test beam.

Cost Matrix

\$k	THGEM	Zig-Zag Pads	TPC Gas Choice	μ -RWELL Studies	Chromium GEM Foils	Ion Back Flow	TimePix (Students)	TimePix (Materials)	TOTAL
BNL		63.0	12.0						75
Stony Brook						42.0	48.5	20.0	110.5
UVA				7.6	7.6				15.25
FIT				8.9	8.9				17.75
DESY							25.0	10.0	35
Bonn							25.0	20.0	45
INFN	50								50
TOTAL	50	63	12	16.5	16.5	42	98.5	50	348.5